Nanoscale

REVIEW

View Article Online
View Journal | View Issue

Cite this: *Nanoscale*, 2017, **9**, 3698

# Nanostructures for NIR light-controlled therapies

Yanmei Yang,*[a] Junxin Aw[b] and Bengang Xing*[b,c]

Received 25th November 2016,
Accepted 20th February 2017

DOI: 10.1039/c6nr09177f

rsc.li/nanoscale

In general, effective clinical treatment demands precision medicine, which requires specific perturbation to disease cells with no damage to normal tissue. Thus far, guaranteeing that selective therapeutic effects occur only at targeted disease areas remains a technical challenge. Among the various endeavors to achieve such an outcome, strategies based on light-controlled therapies have received special attention, mostly due to their unique advantages, including the low-invasive property and the capability to obtain spatial and temporal precision at the targeted sites *via* specific wavelength light irradiation. However, most conventional light-mediated therapies, especially those based on short-wavelength UV or visible light irradiation, have potential issues including limited penetration depth and harmful photo damage to healthy tissue. Therefore, the implemention of near-infrared (NIR) light illumination, which can travel into deeper tissues without causing obvious photo-induced cytotoxcity, has been suggested as a preferable option for precise phototherapeutic applications *in vitro* and *in vivo*. In this article, an overview is presented of existing therapeutic applications through NIR light-absorbed nanostructures, such as NIR light-controlled drug delivery, NIR light-mediated photothermal and photodynamic therapies. Potential challenges and relevant future prospects are also discussed.

## Introduction

At present, targeted disease treatment without damaging healthy tissues or cells continues to be clinically challenging. One of the most essential requirements to achieve such precision medicine is that sufficient therapeutic agent must be selectively delivered to the disease target site. However, most existing therapeutic agents do not discriminate between disease and healthy areas; that is, they are incapable of automatically targeting and localizing at the disease areas. Therefore, strategies regarding how to effectively enhance localized concentration of therapeutic agents and to provide favorable ailing treatment are of great importance in clinical practice and extensive effort is still required for this purpose.[1–4] Various strategies have been developed for targeted therapy by selectively controlling drug delivery at disease sites.[5–11] With the use of nanotechnology, such accurate release of drug

[a]*Center for Molecular Imaging and Nuclear Medicine, School for Radiological and Interdisciplinary Sciences (RAD-X) and Collaborative Innovation Center of Radiological Medicine of Jiangsu Higher Education Institutions, Soochow University, Suzhou, China 215123. E-mail: Bengang@ntu.edu.sg*
[b]*Division of Chemistry and Biological Chemistry, School of Physical and Mathematical Sciences, Nanyang Technological University, Singapore, 637371, Singapore*
[c]*Institute of Materials Research and Engineering (IMRE), Agency for Science, Technology and Research (A*STAR), Singapore, 117602, Singapore*

**Yanmei Yang**

**Junxin Aw**

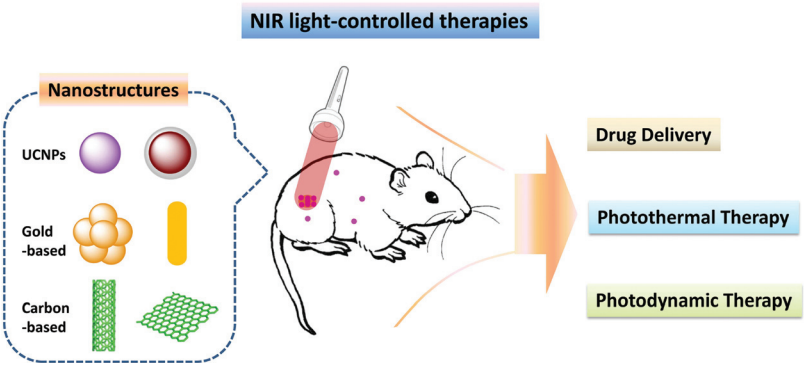


**Fig. 1** Illustration of diverse nanostructures for therapies controlled by NIR light.

molecules at the desired location for selective killing of malicious cells without damaging healthy ones can be accomplished. In traditional terms, many nanocarriers can be used to selectively transport therapeutic agents to disease sites. The non-invasive technique that utilizes external stimulations to control the release of therapeutic molecules on the surface of nanostructures in the targeted area is an ideal therapeutic method. Among proposed external stimuli-induced therapy approaches, those using light irradiation are very interesting. Light as a stimulus is not only low invasive but is also easily controllable in space and time.[12,13]

Currently, great attention is focused on investigations of photo-controlled therapies because light offers remote activation of a wide range of materials (*e.g.*, upconversion nanoparticles (UCNPs), gold-based nanostructures, carbon-based nanomaterials) at a specific time and location with a high precision.[14,15] In general, technical concerns associated with effective photoapplications in biomedical systems include light absorption, scattering, and deep tissue penetration. It is widely accepted that short-wavelength light could potentially induce photoreactions in nucleic acids or proteins, and is thus harmful to living cells.[16,17] Moreover, in the UV or visible range, light may not adequately penetrate tissue because it is easily absorbed and scattered by certain endogenous light absorbers in living systems such as water, lipids and protein molecules, including hemoglobin and oxyhemoglobin,[18–20] which limit *in vivo* therapeutic applications *in vivo*.[21–23] One promising option to overcome these technical obstacles is to use light irradiation in the long-wavelength region, which ranges from 700 to 1000 nm, also known as the NIR window. Living tissues display minimum light absorption in the NIR range, but in the NIR window can penetrate to depths of several centimeters.[24–26] Such a unique optical capability could meet requirements of maximum light transparency and may therefore benefit photo-controlled therapies *in vitro* and *in vivo*.

Thus far, several useful strategies have been investigated for targeted therapies on the basis of NIR light-assisted nanostructures.[27–29] One commonly used approach to achieve such purpose makes use of the photosensitive nanoplatform itself, which can respond to NIR light irradiation or convert NIR light irradiation into short-wavelength emissions, to activate therapeutic cargos on the nanomaterial surface or encapsulated within nanocarrier structures for controlled delivery.[30,31] Another well-established strategy, photothermal therapy (PTT), directly utilizes the photoabsorbing components in the nanostructures that absorb NIR light and then converts photoenergy into thermal effects.[32] Such light-transduced heat can be used to ablate nearby abnormal cells, and thus greatly minimize damage to healthy tissue.[33] The third commonly applied solution is primarily based on the concept of photodynamic therapy (PDT), in which the nanomaterials will conjugate with photosensitizers (PS). Upon NIR light illumination, the PS molecules can generate reactive oxygen species (ROS), and thus achieve the targeted therapeutic effects *in vitro* and *in vivo*.[34] Owing to the numerous advantages of NIR light-assisted therapies, photosensitive nanostructures that are NIR light-responsive have attracted tremendous interest among biomedical researchers. Thus far, many nanomaterials with such light-responsive activity, such as UCNPs, gold-based nanostructures, carbon nanotubes, graphene oxide, and other related materials (*e.g.*, copper sulfide (CuS), molybdenum disulfide ($MoS_2$), black phosphorus (BP)), have been proposed for NIR light-controlled therapies.[24,35–37] In this review, we mainly focus on developments reported in

**Bengang Xing**

the literature over the last five years. We discuss NIR light-mediated drug delivery, NIR light-controlled photothermal treatment and photodynamic therapy with light-processing wavelength ranging from 700 nm to 1000 nm, which is mainly in the first biological NIR window (Fig. 1).[38–40]

## NIR light-controlled drug delivery

NIR light-controlled drug delivery strategies could enhance therapeutic quality by preventing non-target effects through spatiotemporal activation. Approaches for such light-mediated chemotherapy could effectively decrease damage to normal tissues and thus have been intensively investigated in recent years for applications in precision medicine. In the disease treatment process, such NIR light-responsive functional nanostructures not only show promising capacity to penetrate the fenestrated endothelium present in disease areas (*e.g.*, tumor) on the basis of enhanced permeabilization and retention (EPR) effect,[41] but, more importantly, they can also spatiotemporally deliver the therapeutic reagents or specifically activate unique physiochemical properties at the diseased lesion site upon light irradiation at NIR windows.[42] In order to achieve light-controlled drug delivery, rational design based on the NIR light-activated chemical bond or linkage moieties (*e.g.*, thermo-responsive polymer) that have photothermal effect are incorporated into nanoconjugate structures. As such, nanometer-sized structures can also work as delivery "cargos" to improve treatment efficacy by efficiently directing greater concentrations of therapeutic agents into disease areas. Moreover, the promising activation of drug molecules only at the disease site can be spatially controlled by NIR illumination.[43–45] Toward this objective, several types of NIR-responsive, nanostructure-based drug delivery platforms have been extensively studied.[46–50]

### Therapeutic reagent loading forms: non-covalent and covalent interactions

In general, an ideal therapeutic reagent would be expected to carry out multiple functions, where modalities with different functions are integrated into a single entity. This is challenging for conventional molecule design and synthesis. Fortunately, this issue can be addressed with nanostructures because reagents such as target ligands, drug molecules, imaging probes, and photosensitizers can be immobilized into a single nanoparticle through elegant but feasible construction techniques.[51,52] Normally, multiple reagents can be integrated into nanomaterial structures *via* non-covalent bonding and covalent bonding.

For delivery systems based on non-covalent drug loading, the therapeutic molecules may not covalently bond to the nanostructure. In general, on the basis of nanostructure surface morphology, the therapeutic agents could be directly encapsulated within nanomaterials through physical interactions including electrostatic interactions, π–π stacking and hydrogen bonding.[53] In certain cases, the surface morphology of related nanostructures may also need to be modified in order to physically attract the therapeutic reagents or other molecules. For instance, by taking negatively charged DNA and RNA structures, the carrier silica-coated UCNPs can usually be modified with positively charged linkers to electrostatically adsorb DNA/RNA on the surface through coulombic interactions.[54] Another example is the single-layer molybdenum disulfide ($MoS_2$) nanosheets, which were decorated with chitosan (CS) for loading the anticancer drug.[55] Moreover, mesoporous NPs, hollow NPs and polymeric nanomaterials are especially appropriate carriers for such non-covalent based delivery. Benefiting from their high surface-to-volume ratio and pore cavity, these NPs can hold large amounts of therapeutic agents in the structures, and thus can significantly enhance the loading efficiency (Fig. 2a).[56]

The covalent binding is the typical way that a direct chemical bond should be employed for the association between the payloads and the transport vectors.[53] For the light-triggered drug delivery system, the concept of prodrug is normally involved, in which a photoliable chemical linker will be used to covalently link drug molecules within the delivery platform to form prodrug. Upon exposure to light excitation, the drug molecules will be released in a highly-controlled manner and drug activities will be recovered.[7] Since the efficacy of drug release is largely dependent on the linker's response sensitivity to light triggers, the choice of an appropriate covalent linker is extremely important (Fig. 2b).[24] Currently, several photocaged chemical groups including *o*-nitrobenzene (NB),[57,58] pyrenylmethyl ester,[59] coumarinyl ester[60,61] have been well established for spatiotemporally controlled release of therapeutic molecules *in vitro* and *in vivo*.

By taking the photoactive NB derivatives as an example, which are the most commonly used linkage moieties to covalently conjugate drug molecules with nanocarriers, such NB moiety can be cleaved upon UV light illumination to achieve effective drug release.[62] Despite high efficiency for the targeted photocleavage, obvious disadvantages including potential light damage to native biomolecules and its poor penetration ability significantly hinder light-triggered drug delivery in deep

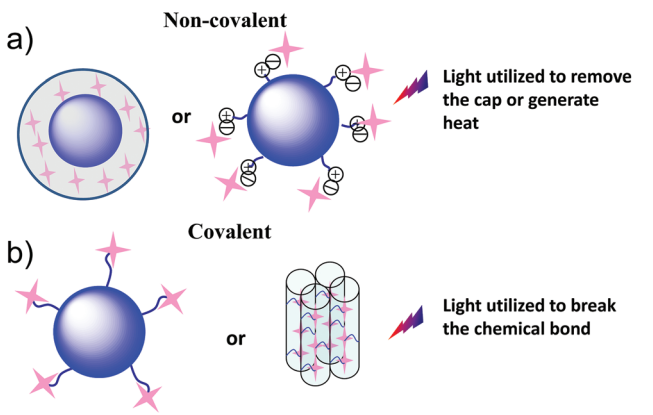


Fig. 2 Schematic diagram illustrating non-covalent (a) and (b) covalent formations of therapeutic reagent immobilization with nano-materials.

tissues. Therefore, alternative approaches to overcome these technical obstacles are highly desirable. One such solution is to rely on long-wavelength light illumination at the NIR window ranging from 700 to 1000 nm.[38–40]

In the following, diverse types of functional nanoplatforms commonly employed for NIR light-responsive drug delivery, including UCNPs, gold-based nanomaterials, carbon-based nanomaterials and other related nanostructures, are systematically introduced.

### Upconversion nanoparticles

In principle, during the process of light-mediated drug activation in biomedical applications, long-wavelength light excitations will be always preferred since they are less detrimental to tissue, and importantly, they have deeper light penetration capability. However, conventional photo-activation of biomolecules and "uncaging" of photolabile moieties may have to rely on short-wavelength light irradiation (*e.g.*, UV or blue light excitation), which usually bears higher energy and therefore may cause cellular damage and limited penetration depth. To overcome this obstacle, alternative designs that can bridge NIR light to UV excitation (*e.g.*, absorb NIR excitation and emit UV emission) are desirable. One promising strategy for such NIR light-responsive drug delivery is through application of UCNPs, which can absorb long-wavelength NIR light illumination and convert them into short-wavelength emissions in the UV to visible range and even to the NIR region.[63] The emitted wavelength light can be controlled through host/dopant combinations and dopant concentrations (*e.g.*, doping with Tm for UV emission).[64–67] Generally, these upconversion processes are often divided into three broad classes: excited stated absorption (ESA), energy transfer upconversion (ETU) and photon avalanche (PA).[68,69] Under continuous-wave (CW) excitation (980 nm or 808 nm), UCNPs often exhibit a large anti-Stokes shift of several hundred nanometers, long lifetimes and excellent photostability.[70–72] This photo-conversion property allows UCNPs to serve as the excitation source for biomedical applications, such as cell imaging,[73–77] optical imaging *in vivo*,[78–85] biosensors[86–91] and bioassays.[88,92,93] More importantly, UCNPs have been suggested as suitable transporters,[94] especially for drug delivery systems based on covalent binding modes.

Due to the special property that can convert NIR light irradiation into shorter-wavelength emissions (normally from UV to visible range), lanthanide-doped UCNPs have attracted tremendous interest in recent years.[26,95] The upconverted luminescence can be used to unblock the photolabile "caging" moiety and reactivate the bioactive molecules in spatial and temporal precision. For example, Xing's group has demonstrated the concept that the use of NIR light (*e.g.*, at 980 nm) could be used to trigger the release of caged D-luciferin based on UCNPs ($NaYF_4$:Yb,Tm).[96] In this typical study, the UCNPs were first coated with solid silica shell (UCNPs@$SiO_2$) to facilitate the increased biocompatibility and subsequent particle surface functionalization. The commonly used photoliable "caging" moieties, *o*-nitrobenzyl, were employed to block D-luciferin, a robust bioluminescent probe for specific recognition of the gene reporter firefly luciferase, and were further covalently linked to the NPs surface. Upon NIR laser irradiation, the caged D-luciferin can be released by one of the converted UV emissions from UCNPs. This novel NIR-controlled uncaging of D-luciferin can react with firefly luciferase to produce photons at 560 nm, which then are used for bioluminescence imaging *in vitro* and *in vivo*. Moreover, a similar approach was also carried out to control release of the anticancer drug 5-fluorouracil, as demonstrated by Fedoryshin *et al.*[97] In prodrug design, the parent drug molecules are activated by UV light excitation. The converted UV emission from NIR-laser excited UCNPs ($NaYF_4$:Yb,Tm) can be used for direct control of drug activities in cancer therapy. Based on this design, several antitumor reagents that indicate light-induced cytotoxicity have been used to conjugate with surface modified UCNPs for the targeted tumor inhibition. For instance, Xing's[98] and Lin's groups[99] have independently developed a novel NIR light-activated drug delivery method based on UCNPs. Typically, in the strategy presented by Xing's group, the unconverted UV emission from UCNPs@$SiO_2$ ($NaYF_4$:Yb,Tm@$SiO_2$) could locally activate the light responsive Pt(IV) prodrug that generates effective antitumor cytotoxicity *in vitro* and *in vivo*. Moreover, the promising antitumor treatment has also been systematically evaluated by multi-modality imaging analysis. Interestingly, based on the process of programmed cell death induced by NIR light-mediated prodrug activation, fluorescence imaging through the cleavable DEVD peptide hydrolyzed by apoptosis-activated caspase-3 enzyme (Fig. 3) has also been applied to evaluate early stages of tumor therapeutic intervention. While in Lin's design, the novel photoactive Pt(IV) prodrug, *trans*, *trans*, *trans*-[$Pt(N_3)_2(NH_3)(py)(O_2CCH_2CH_2CO_2H)$] was conjugated within the core–shell $NaYF_4$:Yb,Tm@$NaGdF_4$:Yb UCNPs complex. This unique prodrug UCNPs nanomedical system exhibited potent *in vivo* antitumor activity after 980 nm laser irradiation. Additionally, it supplies a new way for tri-modality imaging of tumor status and treatment *in vivo*. Besides the unique design to spatiotemporally activate metal-based antitumor drugs, currently a similar concept has been broadly applied to light-mediated release of other conventional antitumor reagents, such as doxorubicin (Dox).[55,56]

Another alternative approach for UCNPs-based, NIR light-controlled drug delivery is to use a mesoporous silica shell to coat the UCNPs surface.[100] Such silica coated-UCNPs provide promising biocompatibility and photostability.[12] For instance, Zhang's group has recently demonstrated application of mesoporous silica-coated UCNPs (NaYF4:Yb,Tm@m$SiO_2$) for remotely controlled delivery of "photocaged" siRNA and DNA moieties.[101] In their work, siRNA or plasmid DNA was caged by a photoactive linkage, 4,5-dimethoxy-2-nitroacetophenone (DMNPE). After the caging process, they were encapsulated into the mesopores with a loading rate larger than 70%. These "caged" nucleic acids can be photo released by the upconverted UV light under 980 nm laser irradiation, and thus achieve spatial and temporal regulation of gene silencing both *in vitro* and in living tissues. Benefiting from more

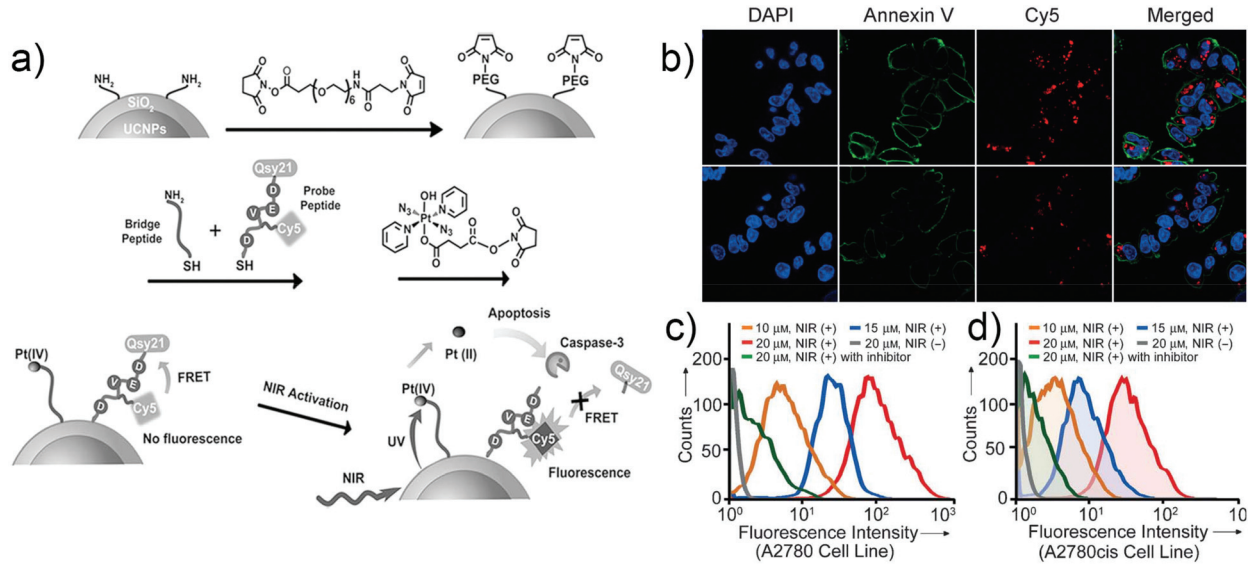


**Fig. 3** (a) Illustration for NIR-light activation of platinum(IV) prodrug based on upconversion-luminescent NPs. (b) Cell imaging of Pt(IV) probe UCNP@$SiO_2$-incubated cells after 1 h NIR irradiation. Two kinds of cell lines used: A2780 cells (first line), A2780cis cells (second line). (c, d) Quantitative flow cytometric analysis of A2780 and A2780cis cells, respectively. Reprint from ref. 98 with permission. Copyright 2014, WILEY-VCH Verlag GmbH & Co. KGaA, Weinheim.

significantly enhanced tissue penetration and minimum light toxicity of NIR light than direct UV light irradiation, the NIR-to-UV-triggered drug delivery platform through UCNPs can serve as a new approach in various fields.

By encapsulating UCNPs in liposomes, Zhang's group recently reported a novel NIR light-triggered drug delivery system.[102] In their work, UCNPs ($NaGdF_4$:Yb,Tm) were encapsulated in azobenzene (Azo)-doped liposome to form the UCNPs@Azo-lipo hybrid vesicles, which can be used for loading the anticancer drug Dox. Upon NIR light (980 nm) irradiation, the azobenzene amphiphilic molecules transform the *trans*-isomer into the *cis*-isomer under converted UV/vis light from UCNPs. This reversible isomerization of the azobenzene group causes movement of the liposome membrane, thereby inducing release of drug molecules.

### Gold-based nanostructures

Noble metal gold-based nanostructures provide a versatile platform for a broad range of applications in biomedicine, especially for the controlled drug delivery. Several representative structures including gold nanorods (AuNRs), gold nanoshells (AuNSs) and gold nanoparticles (AuNPs) have been well studied owing to biocompatibility, easy surface functionalization and tuneable physical properties.[103–106] Typically, when these nanostructures are irradiated with light, the excited electrons rapidly accumulate on their surface, which is known as localized surface plasma resonance (LSPR). Electronic oscillation in the NPs will dampen *via* transferring energy to the environment in the form of heat.[107,108] Such plasmonic property of gold-related nanostructures can be tuned to the NIR region by changing morphology and shape. In this regard, gold-based nanomaterials, such as AuNRs and AuNSs, are very suitable platforms for NIR light-controlled drug delivery due to their strong longitudinal surface plasmon oscillation in the NIR window. Upon irradiation with NIR light at the SPR wavelength region, these nanostructures absorb the photoenergy and subsequently convert to thermal energy, which will modulate the interaction between nanocarriers and payloads, inducing release of drug molecules.[7,109] Generally, two methods are commonly used for NIR light-induced drug delivery based on gold-related nanomaterials. The first strategy is to employ special moieties to trap drug molecules, such as DNA or thermo-sensitive polymers into nanomaterial structures. Another method is directly utilizing the converted heat effect under NIR light irradiation to accelerate the release of drug molecules, which have been initially attached on the nanocarrier surface *via* non-covalent interactions.

AuNRs usually contain two LSPR peaks—one is from transverse-mode plasma absorption around 520 nm and the other is from longitudinal mode absorption. The latter strongly depends on the nanorod shape and can be adjusted to the NIR region by increasing the ratio aspect of nanorods. Recently, Qu and co-workers have developed a NIR light-triggered drug delivery system by using AuNRs.[28] In order to efficiently encapsulate drug molecules into nanostructures and enhance the stability of AuNRs conjugates in the biological environment, AuNRs were coated with a mesoporous silica shell. The as-obtained core–shell NPs were surface-modified with a DNA aptamer moiety aimed at effective capping of fluorophore (FITC) and the antitumor drug Dox. Upon NIR-light irradiation, the local temperature is raised due to the photothermal effect of AuNRs, resulting in opening of the aptamer cover and thus release of entrapped guest molecules. Similarly, another related work by Yeh's group also focused on the

 

design for NIR light-to-thermal-responsive drug release.[110] In addition to aptamer structures, Chen *et al.* also employed thermo- and pH-responsive polymers to achieve the NIR laser-induced drug release (Fig. 4).[111] In their studies, AuNRs were first coated with mesoporous silica shell for loading drug molecules; obtained Au@$SiO_2$ nanoparticles were further encapsulated in thermo- and pH-responsive polymers, which mainly consisted of poly (*N*-isopropylacrylamide) (PNIPAM). Under irradiation of NIR light, this nanocomposite indicated a rapid increase in temperature, and the drug release rate can be easily improved by using enhanced laser power density (*e.g.*, 16 W $cm^{-2}$). The mechanism of NIR light-controlled drug release is mostly attributed to the laser-converted thermal effect of dissociated electrostatic interactions between the drug Dox and polymer shell structures.

In addition to AuNRs, AuNSs can serve as NIR-controlled drug delivery platform because of their excellent NIR-absorption capability. Usually, morphology can be either a hollow gold shell or a composite particle comprising a core (such as a silica seed) packaged by a gold shell. Thus far, several novel designs toward NIR light-controlled drug delivery on the basis of AuNSs have been demonstrated.[27,112,113] By taking the hollow gold nanoshell (HAuNS) as an example, the anticancer drug Dox was loaded on its surface through electrostatic adsorption.[114] Once the aqueous solution of Dox@HAuNS was exposed to 808 nm laser irradiation (5 W $cm^{-2}$), the absorption intensity of Dox in solution was found to increase significantly, indicating effective release of the free drug. Furthermore, this NIR light-responsive nanocarrier can be used in human breast carcinoma cells. For the controlled cells treated with Dox@HAuNS only, the anticancer molecules did not reach the nuclei, suggesting that the Dox drug molecules were not released from the nanoshell. However, when tumor cells were treated with Dox@HAuNS and subsequent NIR laser irradiation, the significant red fluorescence signal was observed in the cell nuclei, which clearly indicated that the drug was released under NIR laser irradiation.

As for most reported materials based on AuNPs, intrinsic size-dependent plasmon absorbance (*e.g.*, 520 nm for 10 nm AuNPs or 580 nm for 100 nm AuNPs) is not directly optimal for NIR light-responsive therapy.[115,116] However, when involved in the process of self-assembly[117–119] or combination with other nanomaterials, AuNPs could also be employed for NIR light-triggered drug delivery. For example, Yang and co-workers[120] synthesized the integrated nanoplatforms by assembling UCNPs into mesoporous silica nanoparticles followed by functionalization with small gold nanocrystals (5 nm ). Upon laser irradiation of the hybrid complex at 980 nm, the green emission from UCNPs overlaps with the plasmon absorbance observed in gold nanocrystals and causes obvious heat generation, which then induces the effective release of the anticancer drugs (*e.g.*, Dox) loaded on the pores of a mesoporous silica nanohybrid structure.

Among gold-based nanomaterials, nanocages (AuNCs) and nanostars have also attracted great attention due to strong absorption in the NIR region.[121] Moreover, hollow interiors and porous walls of AuNCs are suitable for NIR light-induced drug delivery. In 2014, Xia's group demonstrated a NIR laser-responsive delivery of anticancer drug molecules for targeting breast cancer stem cells (CSCs) therapy.[122] In their work, a phase-change material (PCM) was used to encapsulate the drug molecules into the AuNCs. A small molecule SV119, which can bind the sigma-2 receptor on the surface of breast CSCs, was used to functionalize the nanocage surface. Once irradiated with NIR light (808 nm), the heat generated melts the PCM, followed by release of anticancer drug molecules. Recently, Espinosa *et al.*[123] systematically investigated gold nanostar heat-generating efficiency under light irradiation of diverse wavelengths. In their work, three representative gold nanostars (25 nm, 85 nm, 150 nm) were selected to study their photothermal properties both *in vitro* and in living mice. Experimental results indicated that the key factor affecting photothermal therapy efficiency for gold nanostars is size and biodistribution *in vivo*.

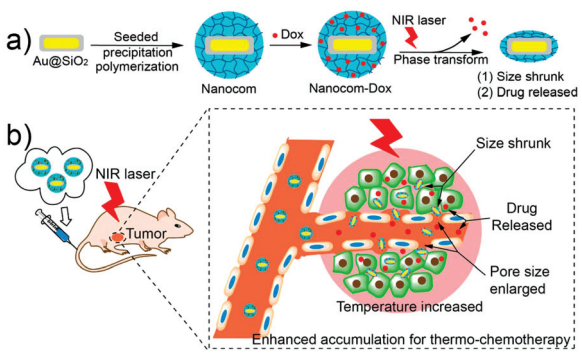


Fig. 4 (a) Schematic illustration of nanocomposite formulation process. (b) NIR laser-induced drug release based on nanocomposite. Reprint from ref. 111 with permission. Copyright 2014, American Chemical Society.

## Carbon-based nanomaterials

Carbon-based nanomaterials, including three main branches according to dimensions—fullerene, carbon nanotube (CNT) and graphene—have attracted great attention for decades in many fields from materials science to biology applications. Typically, carbon-based nanostructures often have favorable sizes, which made them ideal nanocarriers to deliver biomolecules into the target area.[124] CNT and graphene materials have been extensively studied in the biomedical sciences, mostly due to their intrinsically strong NIR optical absorbance (700–1000 nm).[108,125–132] Similar to gold nanomaterials, carbon-based nanostructures can efficiently absorb NIR light and the photoenergy is released in the form of heat.[133,134] In this context, our principal focus is on carbon-based nanomaterials for NIR-controlled drug delivery, including CNT and graphene derivatives.

Major development of CNT platforms in biomedicine has taken place in recent years.[135,136] Qin *et al.*, for instance, reported a Dox-delivery system through functionalized CNT with the surface coated by amphiphilic biopolymer.[137] In this study,

the CNT were first functionalized with biopolymer CS through hydrophobic alkyl chains. The platform was further encapsulated into thermal-sensitive poly(*N*-isopropylacrylamide) (PNIPAAm) material structures. For the *in vitro* release studies, HeLa cells were incubated with Dox-loaded CS/PNIPAAm@CNT nanoparticles for various time periods (*e.g.*, 15 min, 2 h and 24 h). After NIR laser irradiation ($\lambda$ = 808 nm, 1 W cm$^{-2}$), the hybrid CNT materials could induce rising temperature, which subsequently initiated the Dox release. Meanwhile, the fluorescence intensity of Dox was also found to increase, which clearly indicated that NIR light excitation could effectively trigger release of drug molecules from CNT structures.

More recently, the 2D graphene structures have also emerged as novel nanomaterials in biomedical fields attributed to their promising optical functions, good biocompatibility and large surface area. Graphene usually demonstrates its high absorption in the NIR window, and has thus been widely utilized as a remote trigger to control drug delivery. In 2011, Zhong and co-workers[138] fabricated Dox-loaded PEGylated nanographene oxide (Dox-PEG-NGO) for chemotherapy. Generally, drug molecules were loaded on the surface of nanographene oxide through the simple π–π stacking. The *in vivo* antitumor treatment based on Dox-PEG-NGO nanocarriers was conducted by NIR light illumination (2 W cm$^{-2}$) for 5 min, the tumor was found to be completely destructed without obvious weight loss or recurrence of mice body weight. Moreover, Matteini *et al.* also reported that graphene could be employed for NIR light-controlled drug release.[139] In this kind of NIR light-controlled drug delivery systems, graphene and its derivatives have been known to play the dual roles as a temporary storage for drug delivery or as an effective transducer to convert NIR light into heat that induces drug release.

### Other nanomaterials

Besides UCNP materials, gold-based NPs and nano-size carbons, many other new types of materials such as copper sulfide (CuS) and $MoS_2$ nanostructures that are capable of responding to NIR light have also been designed recently for light-controlled drug release *in vitro* and *in vivo*.

For instance, Liu *et al.* reported a facile, cheap and green method for the synthesis of mesoporous silica-coated copper sulfide nanoparticles (CuS@m$SiO_2$), which were used as an effective NIR light-responsive platform for controlled drug delivery.[140] Under NIR laser (*e.g.*, at 980 nm, 0.72 W cm$^{-2}$) irradiation, the anticancer drug Dox is released from nanocomposites mainly due to the locally elevated temperature that promotes effective drug diffusion.

Apart from carbon-based graphene and its derivatives, a new type of 2D nanomaterials has also emerged in the nanomedicine field partially because of their large surface area, an ideal template to adsorb a large quantity of drug molecules. A representative example is the single-layer $MoS_2$,[141] which was first synthesized by chemical exfoliation in 2011.[142] In 2014, Zhao and co-workers demonstrated a simple and low-cost approach for NIR light photothermal-triggered drug delivery.[55] Typically, the commercially available $MoS_2$ are treated with oleum and sonicated to form a grayish dispersion. To increase water solubility of $MoS_2$ nanosheets, CS biopolymer is introduced to functionalize the $MoS_2$ nanosheets. The commonly used anticancer drug Dox is non-covalently loaded onto the $MoS_2$-CS complex by mixing with the solution containing $MoS_2$ (Fig. 5). In a typical cellular study, KB cells are incubated with $MoS_2$-CS-Dox for 2 h. Upon NIR light irradiation, the red fluorescence signals inside cells are found to be greatly enhanced, suggesting that the Dox is released from the $MoS_2$ nanosheets. Results of many additional studies carried out *in vivo*, and compared with control experiments, clearly reveal that tumor growth was effectively inhibited after treatment with $MoS_2$-CS-Dox under NIR-laser irradiation.

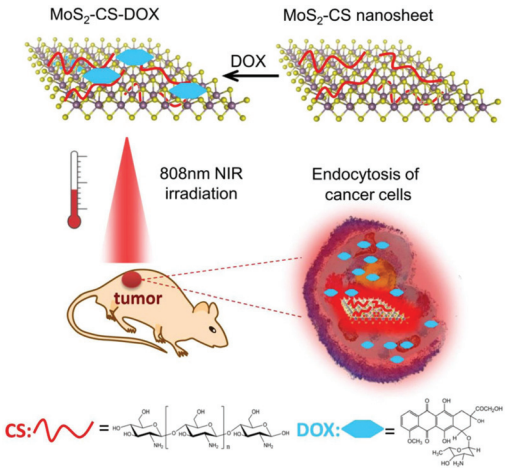


**Fig. 5** Schematic illustration of Dox-loaded, single-layer $MoS_2$ nanosheets and NIR light-induced drug release in the tumor site. Reprint from ref. 55 with permission. Copyright 2014, American Chemical Society.

## NIR light-controlled photothermal therapies

Photothermal therapies have shown great promise in recent years, especially for tumor treatment *in vitro* and *in vivo*. In general, PTT employs photothermal agents to absorb light and then converts it into heat energy. Some NPs dissipate the absorbed energy, releasing heat into the surrounding space upon exposure to an NIR laser beam.[53,143] Such process leads to overheating the local area, which results in an increased capability for membrane permeability and/or promotes the destruction of biological material (such as protein denaturation) and causes subsequent cell death.[144] Typically, as an effective PTT therapeutic agent for killing tumor cells, the targeted photoresponsive temperature enhancement (*e.g.*, ~45 °C) is essential for effective light irradiation.[145] Additionally, in order to guarantee heating precision, a targeted and multifunctional PTT agent is often used in imaging-guided photothermal therapy (*e.g.*, photoacoustic imaging, MR imaging and fluorescence imaging).[146,147]

 

Apparently, the ideal light source for controlling targeted *in vitro* and *in vivo* PTT is in the NIR region, which has been known to indicate higher penetrating capability and cause minimal side effects in biological tissues when compared to UV light. Several types of photosensitive nanostructures, such as selected nanocomposites, gold-based nanostructures[148] and carbon nanotubes, have been widely developed and employed in PTT. All of these nanomaterials have been known to uniformly possess intense absorption bands in the NIR window ranging from 700 nm to 1000 nm.

### Upconversion nanoparticles

Unlike gold-related nanostructures that utilize strong NIR absorbance to convert light directly into heat to inhibit cancer cell growth, UCNPs (lanthanide-doped nanomaterials) are rarely used directly as PTT agents.[83,149] However, when UNCPs are combined with other plasmonic nanostructures, such as Au,[93] Ag[150] and $Fe_3O_4$,[151] resulting hybrid nanocomposites exhibit high efficiency as seen in reports for PTT cancer therapy *in vitro* and *in vivo*. In addition to plasmonic nanomaterials, other optics-absorbing agents including CuS and NIR-absorbing dye molecules are reported to integrate with UCNPs structures for light-controlled biomedical applications. For example, Shi *et al.* demonstrated a new type of silica-coated UCNPs ($NaYbF_4$:Er, Tm@$SiO_2$) nanocomposites by surface functionalizing with ultra-small CuS NPs for photothermal therapy.[152] The CuS NPs were employed as photothermal agents to convert light to heat effects. When the nanocomposite solution (1.2 mg $mL^{-1}$) exposed under 980 nm laser illumination (*e.g.*, 1.5 W $cm^{-2}$, 5 min), the temperature was increased from 25 °C to 40 °C. Upon intratumor injection of designed therapy agents into 4T1 cells-bearing mice for 1 h and followed by 980 nm NIR laser irradiation, tumor growth was found to be significantly inhibited, which confirms the great potential of such UCNP-CuS agents for photothermal treatment *in vivo*.

Thus far, most reported NIR light-controlled therapy strategies based on UCNPs rely mainly on light illumination at 980 nm. Such long-wavelength light works efficiently, but it may directly overlap with water absorption,[153] and thus may cause several unwanted outcomes such as overheating that damages tissues. Fortunately, several approaches were developed that avoid these results, such as a new type of UCNPs that can be excited by shorter-wavelength light, say, at 800 nm,[154,155] or coating UCNPs with NIR-absorbing molecules.[156] For example, Liu and co-workers[40] developed a multifunctional UCNP-based nanoplatform ($NaGdF_4$:Yb,Er) by loading two types of fluorescent dye molecules, including an NIR-absorbing dye (IR825) and a photosensitizer dye (Rose Bengal, RB) into the UCNP surface. After 808 nm laser irradiation for 5 min, the temperature was found to rapidly increase from 20 °C to 43 °C *in vitro* (with light dosage of 0.5 W $cm^{-2}$), and from 30 °C to 45 °C *in vivo* (dosage of 0.35 W $cm^{-2}$).

### Gold-related nanomaterials

Gold nanomaterials are ideal PTT agents because of their strong light absorption in the visible and NIR regions, as previously mentioned. In principle, absorbed light energy can be converted into heat effects, which subsequently release in the surrounding media (called "photothermal effect") and are capable of destroying nearby biological structures. Moreover, gold nanomaterials have been found to exhibit other excellent properties for biomedicine applications including reasonable photostability and good biocompatibility. Thus far, strategies for photothermal therapy based on gold nanomaterials are very encouraging.

As early as 2003, Lin and co-workers reported using AuNPs as a photothermal sensitizer in PTT.[157] In their work, pulsed laser has been used to induce heat in cancer cells treated with AuNPs. The light-mediated PTT operation showed highly localized photothermolysis of the targeted cells. Since then, a few other groups have independently reported the use of gold nanomaterials in PTT treatment triggered by long-wavelength light illumination.[158–160] In 2013, Chen's group proposed a novel route to construct a biodegradable plasmonic gold nanovesicles for both PTT and PA studies.[161] As shown in Fig. 6, gold nanovesicles were prepared by assembling AuNPs tethered with an amphiphilic block copolymer, poly(ethylene glycol)-*b*-poly(ε-caprolactone) (PEG-*b*-PCL). The gold nanovesicles showed strong absorption in the NIR region and demonstrated enhanced photothermal efficiency upon 0.5 W $cm^{-2}$ or 1 W $cm^{-2}$ laser irradiation *in vivo* (*e.g.*, with temperature change ($\Delta T$) of 18 °C after 808 nm laser irradiation of sample at 400 μg $mL^{-1}$, 50 μL, for 5 min). These assembled gold nanovesicles were also found to gradually collapse into discrete AuNPs structures in a temperature- and time-dependent manner, which improved clearance of the gold nanoparticles from the body after phototherapy. In addition to coating with polymers, AuNPs can be assembled with other inorganic nanomaterials for combined PTT. For example, Su *et al.* reported a gold nanoparticles-based NIR hyperthermia agent *via* decorating AuNPs with silicon nanowires

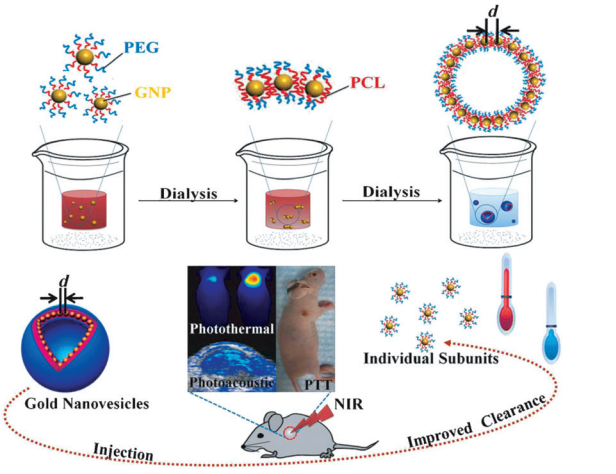


Fig. 6 Schematic diagram illustrating formation of biodegradable gold vesicles, which can serve as PTT and photoacoustic (PA) imaging agents. Reprint from ref. 161 with permission. Copyright 2013, Copyright 2013, WILEY-VCH Verlag GmbH & Co. KGaA, Weinheim.

(AuNPs@SiNWs).[162] The synthesized SiNWs@AuNPs possessed strong NIR absorbance from 700 nm to 1000 nm and displayed excellent heat production upon 2 W $cm^{-2}$ of 808 nm laser illumination for 3 min (temperature change ($\Delta T$) value is ~38.3 °C with concentration of AuNPs@SiNWs samples at 150 μg $mL^{-1}$). Moreover, these hybrid nanomaterials were found to have anti-tumor capacity at concentrations as low as 150 ppm.

AuNRs are also promising candidate nanomaterials for PTT applications because they are easily synthesized and possess strong optical extinctions in the NIR region.[32] AuNRs can be easily fabricated with an aspect ratio of 4 by using the seed-mediated method, which shows promising longitudinal absorbance at approximately 800 nm.[24,163] By taking advantage of this unique property, the nanorod materials can be applied to induce thermal ablation when illuminated by an 800 nm laser. Currently, several strategies have been demonstrated by conjugating AuNRs with other biomolecules for PTT treatment. For example, EI-Sayed *et al.* reported *in vitro* molecular imaging studies with the combination of photothermal cancer therapy by using AuNRs conjugated with anti-epidermal growth factor receptor (anti-EGFR), which selectively binds to malignant cells.[164] In another *in vivo* photothermal system, Maltzahn *et al.* utilized polyethylene glycol (PEG) to stabilize AuNRs.[165] They found that the PEG-AuNRs complex could be dispersed in various solvents and exhibited long circulation half-life *in vivo* (*e.g.*, $t_{1/2}$ ~17 h). Furthermore, these PEG-protected AuNRs exhibit superior photothermal efficiency when injected into tumors of mice. Upon 2 W $cm^{-2}$ of NIR laser irradiation at 810 nm for 5 min, the temperature of the targeted area was rapidly increased to over 70 °C. This platform of AuNRs converting NIR light to heat showed encouraging therapeutic efficacy, as tumors were successfully annihilated within 10 days.

### Carbon-based nanomaterials

Carbon nanomaterials, such as 1D CNT and 2D graphene, have also been commonly used as photothermal agents because of their strong light absorbance in the NIR region, which can cause *in situ* photothermal effects for NIR light-induced photothermal therapy.[124] As early as 2005, for the first time Dai's group demonstrated that CNT could be used for *in vitro* PTT.[39] In summary, DNA-conjugated, single-walled CNT showed high photothermal sensitivity to HeLa cells and induced remarkable cell death rates because solution temperature increased to 70 °C after 2 min of 808 nm laser irradiation (with power density of 1.4 W $cm^{-2}$). Furthermore, the PEGylated CNTs were functionalized with folate acid (FA), which showed high selectivity for cancer cells over those of normal cells with specific tumor markers, thus allowing specific destruction of tumor cells through NIR laser irradiation. In continuation of the effective PTT treatment through the CNTs-based nanoplatform, many research breakthroughs were constructed for further relevant applications in photothermal treatment. For instance, Moon *et al.* developed a biocompatible PEGlyated single-walled carbon nanotube (PEG-SWNT) for NIR-irradiated PTT *in vivo*.[166] Another work by Zhang *et al.* demonstrated a novel strategy for simultaneous assembly of peptide-modified multi-walled CNTs in the presence of NIR light.[167] Therefore, more targeting multi-walled CNTs could be attracted into the tumor and finally achieved effective photothermal cancer treatment. Since then, many studies aimed at providing potent CNTs for their photothermal applications *in vitro* and *in vivo* have been carried out.[166–170]

Recently, in a study by Liu and co-workers, PEGylated nanographene oxide (GO) with fluorescent labeling was first investigated for *in vivo* photothermal therapy (Fig. 7).[171] By conjugating NIR fluorescent dye to GO, the complex showed high tumor-passive uptake in three different tumor models—4T1, KB and U87MG tumor-bearing nude mice. Importantly, they demonstrated that nano-GO is an efficient photothermal agent for generating heat under 808 nm laser irradiation (*e.g.*, 2 W $cm^{-2}$) and thus effectively inhibits tumor growth.

### Other nanomaterials

Gold- and carbon-based nanomaterials and certain other nanomaterials (*e.g.*, BP, CuS, Pd nanosheets) with high optical absorption in the NIR region have also been investigated for applications of targeted PTT *in vitro* and *in vivo*.

BP is a new member of 2D nanomaterials, which is expected to be an attractive theranostic agent, mostly due to its biocompatibility and can degrade to nontoxic phosphate and phosphonate in aqueous media.[172,173] Very recently, Shao *et al.* designed a biodegradable NIR-responsive photothermal ablation cancer treatment strategy using BP-based nanospheres.[174] In their work, the BP quantum dots (~3 nm) were incorporated in PLGA to form BPQDs/PLGA nanospheres for prolonging blood circulation time in the body. Such composite nanomaterials exhibit higher NIR absorbance, which is useful for PTT (Fig. 8). Due to the remarkably enhanced tumor accumulation of BPQDs/PLGA resulting from the EPR effect, photothermal ablation with excellent therapeutic outcomes was achieved in animal experiments.

CuS NPs can be synthesized by using $CuCl_2$ and $Na_2S$ reaction with the optical absorption band in the NIR range.[175] In 2010, Li and co-workers reported *in vitro* and *in vivo* studies by using PEGylated CuS as a photothermal coupling agent for PTT. The thermal effect of PEG-CuS NPs aqueous solution was first examined under 808 nm laser (16 W $cm^{-2}$) irradiation for 5 min, and solution temperature subsequently increased to 80 °C. Moreover, U87 human glioma cells treated with PEG-CuS were also investigated upon irradiation with NIR laser and substantial reduction of cell numbers was observed. Importantly, PEG-CuS was injected into living mice bearing the U87 tumor and followed by 24 h accumulation. The tumor was then irradiated with 808 nm diode laser (12 W $cm^{-2}$, 5 min) and substantial tumor destruction was achieved. In addition to CuS,[176] several other types of copper chalcogenide have been explored for PTT therapy, such as super-CuS,[177] CuSe,[178] CuTe,[179] and the hybrid $Fe_3O_4$@$Cu_{2-x}S$ core–shell NPs.[180]

 

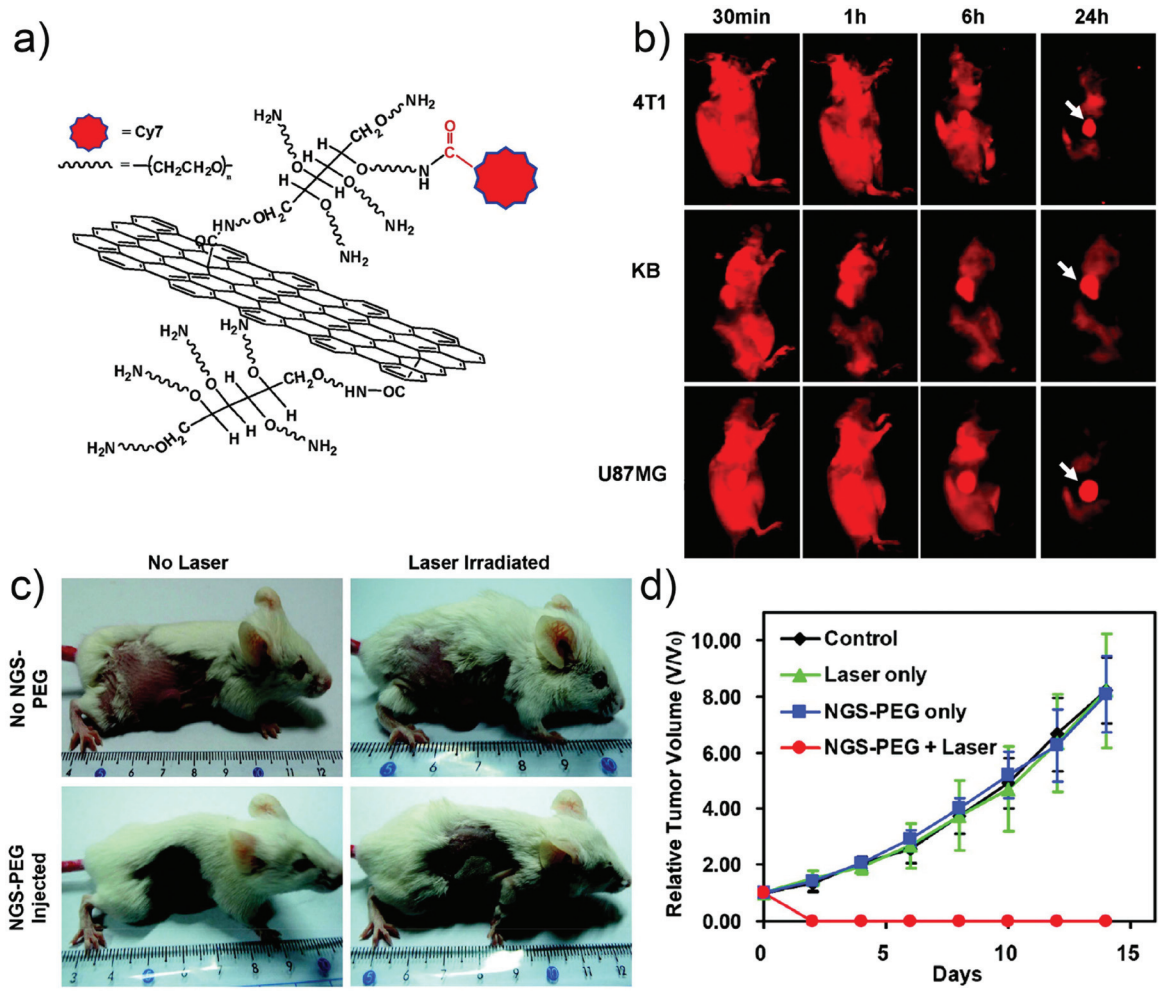


Fig. 7 (a) Scheme of Cy7 labelled, PEGylated-nanographene oxide sheets. (b) *In vivo* fluorescence images of 4T1 tumor bearing-Balb/c mice, KB and U87MG tumor-bearing nude mice taken at various time points (30 min, 1 h, 6 h, 24 h) post-injection of Cy7 labelled, PEGylated-nanographene oxide. (c) Representative photos of mice after various treatments indicated. (d) 4T1 tumor growth curves of various groups after treatment indicated. Reprint from ref. 171 with permission. Copyright 2010, American Chemical Society.

Very recently, other noble metal-based nanomaterials, such as Pd nanosheets, have also attracted great attention as another alternative for photothermal application. Different from conventional noble metal nanomaterials (*e.g.*, AuNPs or AuNRs), which may suffer from potential decomposition and morphology change upon laser irradiation,[180] compared to gold nanostructures, Pd nanosheets exhibit promising stability and thus can serve as reliable agents for PTT disease therapy. For example, Zheng and co-workers reported the synthesis of freestanding hexagonal Pd nanosheets, which demonstrated a well-defined and tunable surface-plasmon resonance peak in the NIR region.[181] These Pd nanosheets exhibit good photothermal stability and thus induce a strong photothermal effect for killing cancer cells.[145,182] Zheng's group also reported the combination of Pd nanosheets with mesoporous silica or drug-loaded mesoporous silica for NIR-induced PTT treatment; significant breakthroughs for effective tumor inhibition have thus been achieved.[183–185]

## NIR light-controlled photodynamic therapies

In contrast to PTT, which utilizes photothermal heat accumulation to induce disease ablation, PDT is a unique type of therapeutic modality that relies on photosensitizer agents to generate ROS under light illumination, such as singlet oxygen ($^1O_2$), which are usually associated with oxidative stress and subsequently cause cell damage.[186] Normally, three key components are essential in a PDT system: a PS molecule, oxygen and a light source that excites the PS. Under light irradiation, the generated free radicals from PS agents oxidize bio-macromolecule components in cells, such as DNA, certain enzymes or proteins, which induces cytotoxicity and kills the cells.[187] Thus far, PDT treatment has been recognized and approved by the FDA for cancer treatment in clinics. In general, the PS agents employed in conventional PDT are molecules that

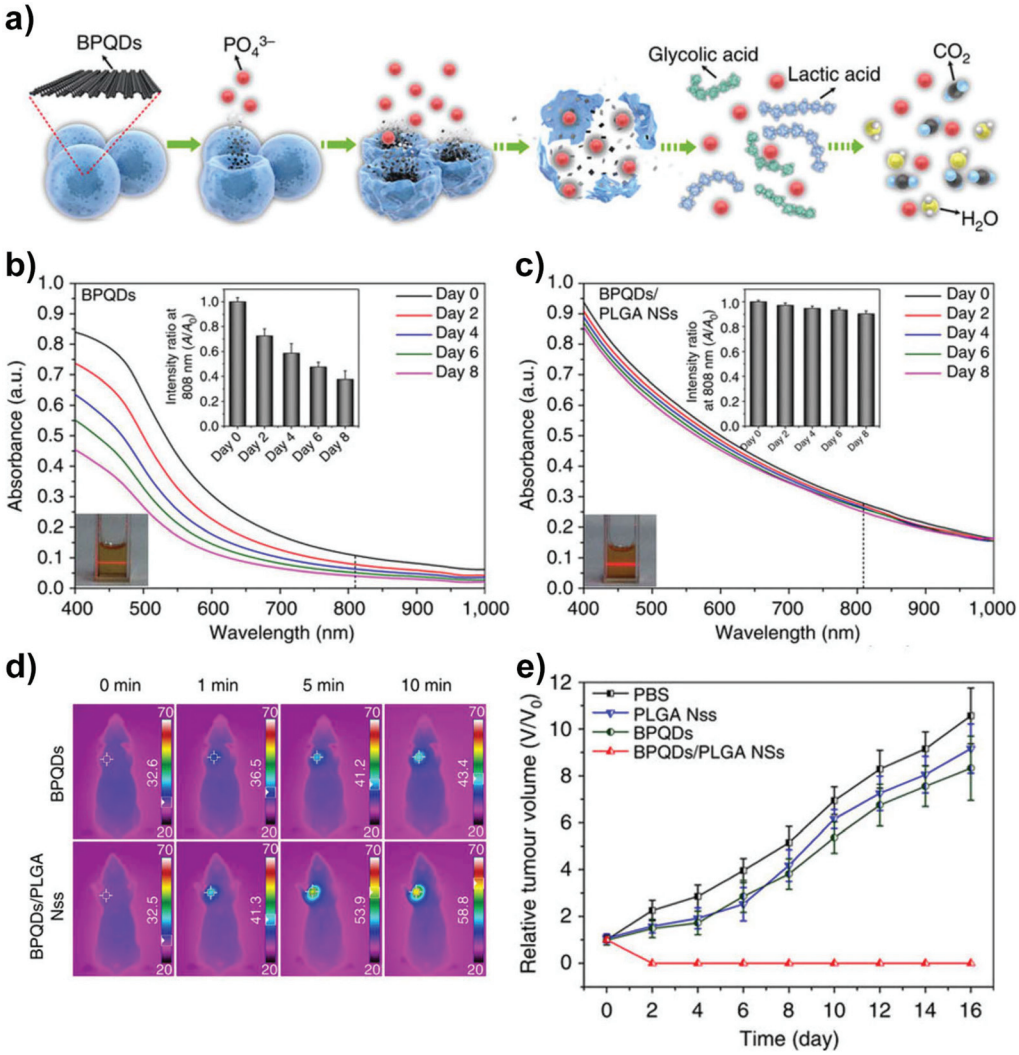


**Fig. 8** (a) Schematic representation of degradation process for BPQDs/PLGA nanospheres. (b, c) Absorption spectra of BPQDs and BPQDs/PLGA nanospheres with same amount of BPQDs at different periods of time (d) Thermographic imaging of BPQDs (top) and BPQDs/PLGA (bottom) injected mice bearing tumors (24 h after injection), irradiated by 808 nm laser (1 W $cm^{-2}$). (e) Tumor growth curves of different groups after effective PTT treatment upon 808 nm laser irradiation. Reprint from ref. 174 with permission. Copyright 2016, Nature Publishing Group.

contain porphyrins or analog structures. As a consequence, most of the PS agents are hydrophobic. Typically, they have poor water solubility and lack effective selectivity/accumulation at the disease target site. In order to overcome these obstacles and meanwhile to improve therapeutic efficacy of PS agents, many nanostructure carriers have been proposed to facilitate the targeted PS agent delivery for PDT in living systems.

Recently, extensive effort has been invested in exploring the feasibility of PDT bio-applications through long-wavelength NIR light irradiation, mostly due to its capability for deeper tissue penetration.[188,189] The usage of NIR light-responsive PDT could significantly improve the safety of PDT treatment. It can effectively reduce light-induced cytotoxicity and minimize possible photosensitivity to ambient light illumination. Many kinds of nanomaterials, including organic NPs (such as liposomes,[190,191] micelles[192–194] and other polymeric NPs[195–197] and inorganic NPs) (such as UCNPs,[29,198–201] gold-based NPs,[202–204] carbon-based NPs,[170,205–210] silica NPs[211,212] and magnetic NPs[213,214]), have been widely explored for both *in vitro* and *in vivo* PDT applications. In this section, we focus mainly on the introduction of UCNPs, gold-related nanomaterials and carbon-based nanostructures for NIR light-induced PDT applications.

### Upconversion nanoparticles

Lanthanide-doped UCNPs, which can convert NIR light into UV or visible light to active several kinds of PS molecules, exhibit great promise in NIR light-controlled PDT applications. In 2007, Zhang *et al.* first demonstrated that UCNPs could be used for *in vitro* PDT to effectively kill cancer cells.[198] In their experiment, UCNPs ($NaYF_4$:Yb,Er) were coated with a porous, thin layer of silica shell to enhance biocompatibility. The PS, merocyanine-540 (MC540), was then loaded into the porous shell. When excited with NIR light (*e.g.*, 974 nm), MC540

 

produces $^1O_2$ and other ROS from the converted UV emission. By conjugating antibody to MC540-coated UCNPs, effective cancer targeting was further indicated as well as high PDT efficiency for destruction of cancer cells. Inspired by this pioneering study, many groups investigated UCNP-based PDT *in vitro* and *in vivo* applications by combining photosensitizers as PDT agents.[40,199,215] For example, Zhang's group designed an *in vivo* PDT approach by using mesoporous silica-coated UCNPs ($NaYF_4$:Yb,Er@m$SiO_2$) with surface loading by two PS molecules (MC540 and zinc(II) phthalocyanine (ZnPc)).[215] The two PS are activated at the same time by multicolored emissions from UCNPs under 980 nm light, which improves generation of $^1O_2$ and notably enhances PDT efficiency. In addition, Gu and co-workers reported an *in vivo* tumor-targeted PDT using UCNPs ($NaYF_4$:Yb,Er) loaded with ZnPc.[25] In their study, UCNPs were coated with folate-modified amphiphilic chitosan (FASOC) and hydrophobic ZnPc molecules were loaded into the DASOC layer. Mice bearing s180 tumors were intravenously injected with FASOC-UCNP-ZnPc and then irradiated with 980 nm light at 24 h postinjection (0.2 W $cm^{-2}$, 30 min). After laser treatment, tumor growth was greatly inhibited as compared to the control group in which the mice were treated with saline. By loading the same PDT agents with ZnPc, Huang *et al.* proposed a 915 nm-light-triggered PDT by using the intensively red-emitting UCNPs ($Na_{0.52}YbF_{3.52}$:Er@$SrF_2$).[216] This kind of ZnPc-loaded UCNPs showed great potential for multimodal imaging (MR/CT)-guided PDT for cancer. Furthermore, the tumor interior is usually not oxygenated adequately (often termed as tumor hypoxia) because tumor tissue often rapidly outgrows its blood supply, resulting in insufficient concentration of oxygen.[217,218] So far, tumor hypoxia has been recognized as one of the crucial reasons for the poor prognosis of many anticancer therapeutics. To resolve this issue, interesting investigations focused on controlling the distance of PS agents with UCNPs or by co-conjugation of hypoxic-sensitive, bio-reductive prodrug (*e.g.*, tirapazamine, TPZ) were also recently proposed. Enhanced PDT tumor treatment within deeper tissue, where the environment is highly hypoxic, can be easily achieved.[219–221]

Very recently, a new type of dye-sensitized UCNPs, which can be excited under a shorter wavelength around 800 nm light by doping the lanthanide UCNPs structures with the $Nd^{3+}$ element, has been developed.[86,154,222–225] Extensive *in vitro* and *in vivo* experiments have clearly confirmed that the shorter-wavelength laser illuminations near 800 nm not only exhibit more robust NIR light-controlled diseases treatment and imaging, but also greatly minimize laser-induced local overheating effects as compared to those done by 980 nm laser excitation.[155,226–228] By using this promising advantage, Xing *et al.* demonstrated a novel tumor micro-environment-responsive UCNP ($NaYF_4$:Yb,Er,Nd@$NaYF_4$:Nd)-based nanoplatform with conjugated surface and protease enzyme-sensitive peptide (Fig. 9a).[229] Upon tumor-specific enzyme reactions, the activated peptides sequence could trigger the covalent cross-linking of neighbouring particles that specifically induced self-accumulation of UCNPs at the tumor site. After 808 nm laser irradiation, such enzyme-triggered UCNP cross-linking would lead to increased upconversion emission and subsequently

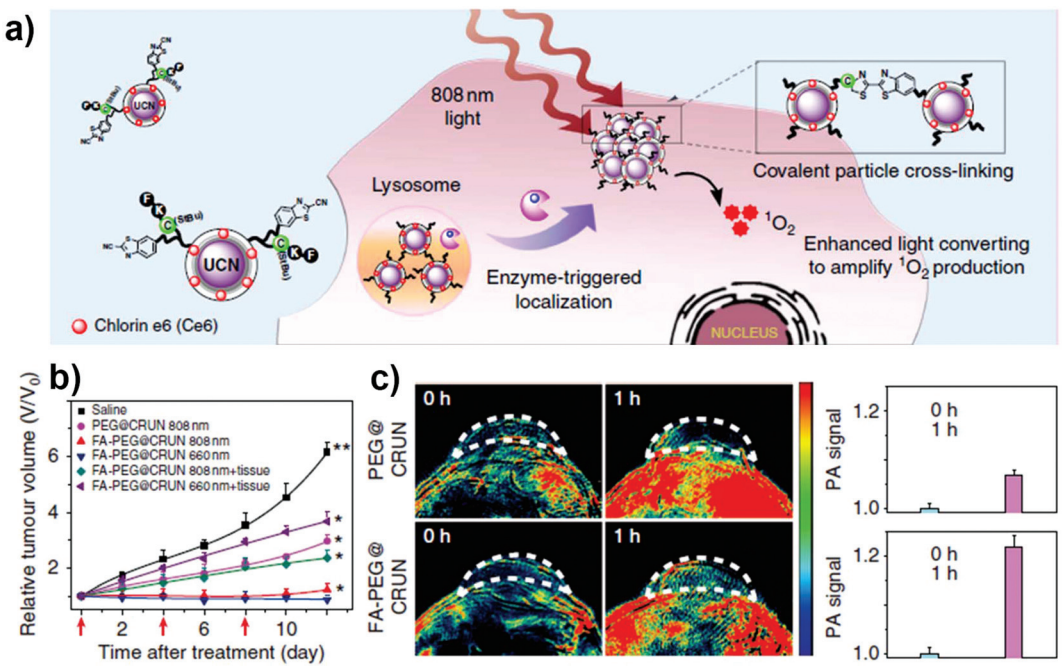


**Fig. 9** (a) Illustration of enzyme-triggered covalent cross-linking of peptide-modified UCNPs for tumor localization and theranostics. (b) Tumor growth curves of various groups after effective PDT treatment under 808 nm laser irradiation. (c) Photoacoustic imaging signals at tumor site after intravenous injection. Reprint from ref. 229 with permission. Copyright 2016, Nature Publishing Group.

amplified ROS generation, which greatly enhanced PDT treatment (Fig. 9b) and multimodality cancer imaging, including *in vitro* and *in vivo* optical and photoacoustic imaging (Fig. 9c).

### Gold-related nanomaterials

Many recent studies clearly reported that combination of AuNPs and organic photosensitizers can enhance PDT treatment effects upon NIR irradiation to effectively kill cancer cells.[202–204,230,231] So far, there are two kinds of established gold nanostructure-based PDT platforms: first, gold nanostructures can serve as reliable nanocarriers for effective PS agent delivery to efficiently achieve increased targeting accumulation. For example, Cheng *et al.* recently designed an NIR-light triggered PDT system by immobilizing PS, Pc 227, on an AuNPs surface *via* the Au–S bond.[202] The AuNPs were stabilized with PEG to improve biocompatibility, and the loading ratio of Pc 227 molecules onto AuNPs surface was controlled at 40 : 1. Upon irradiation with NIR light, the AuNP-Pc 227 conjugates showed efficient PDT inhibition of cancer cell growth. Second, different from the nanocarrier system with PS-agent surface coating, gold nanostructures directly generate ROS under light irradiation, without resorting to PS agents. Recently, Vankayala *et al.*[232] presented this interesting concept by using AuNRs alone that can sensitize formation of singlet oxygen. In their work, AuNRs coated with cationic lipids directly act as activatable PDT agents, which was investigated at the cellular level. Under NIR light irradiation, the platform successfully inhibited the growth of melanoma tumors without any conjugation of photosensitizers. In addition, high performance of this AuNRs-mediated PDT effect was demonstrated for *in vivo* experiments. After administration with lipid-coated AuNRs and followed by laser irradiation at 915 nm (with the power density of 130 mW $cm^{-2}$), B16F0 melanoma tumors in living mice were found to be completely destroyed.

### Carbon-based nanomaterials

As described previously, carbon-based nanomaterials normally demonstrate strong optical absorption in the NIR region and have been widely used for *in vitro* and *in vivo* PTT studies. Moreover, these carbon-based nanomaterials also serve as effective carriers to deliver PS agents and chemotherapeutic drug molecules, and thus promote unique applications in PDT and chemotherapy.

For instance, carbon nanotubes have been used for loading PS molecules such as chlorine e6 (Ce6)[208] and ZnPc[205] through non-covalent interaction. Moreover, Chao's group recently combined luminescent Ru(II) polypyridyl complexes with SWCNT.[170] The Ru(II) polypyridyl complexes would be released from SWCNT through photothermal effect, and meanwhile they produced $^1O_2$ upon double photo-laser irradiation (at 808 nm) (Fig. 10a). The *in vitro* experiment indicated that 808 nm light irradiation (0.25 W $cm^{-2}$, 2 min) of HeLa cells, which were treated with Ru@SWCNTs and 2,7-dichlorodihydro fluorescein diacetate (DCFH-DA), led to significant fluorescence enhancement, suggesting that the DCFH-DA indicator was oxidized by the generated $^1O_2$ in living cells.[233] Furthermore, the *in vivo* examination also demonstrated that the 15-day treatment through tail vein injection of Ru@SWCNTs samples into nude mice bearing the HeLa tumor model and followed by 808 nm laser irradiation (0.25 W $cm^{-2}$, 5 min) resulted in significant tumor ablation in living animals (Fig. 10b).

Similarly, graphene oxide can also be non-covalently functionalized with photosensitizers for PDT applications.[210,234,235] In addition to abovementioned studies, attempts were made to enhance therapeutic efficiency. For example, in 2013, Zhang's group developed a nanocomposite by combining UCNPs with graphene oxide through covalent bonding.[236] The photosensitizer ZnPc was loaded on the nanocomposite surface through

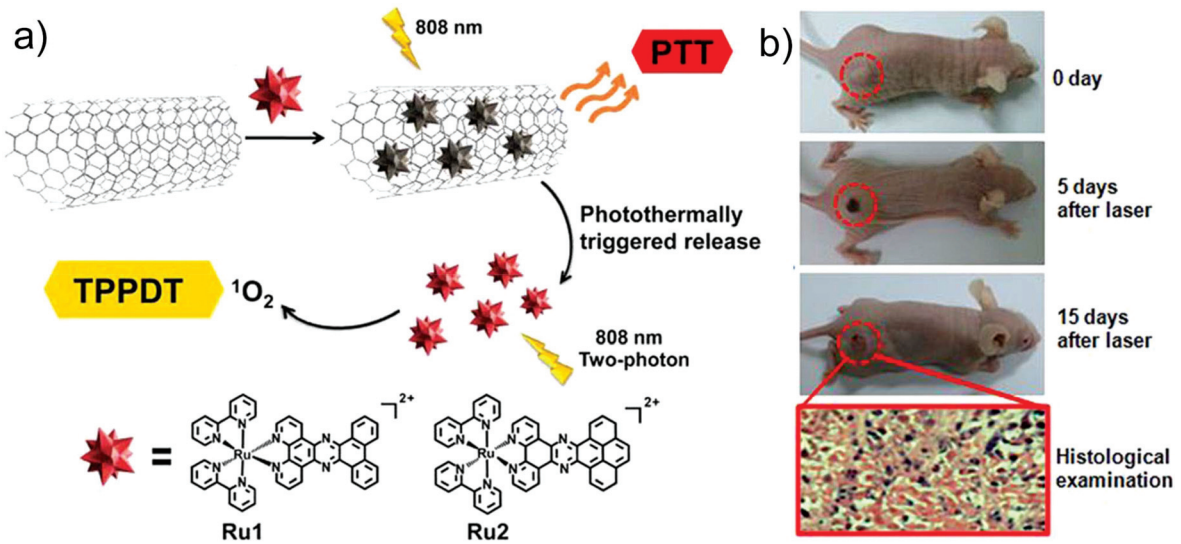


Fig. 10 (a) Schematic illustration of Ru@SWCNTs for NIR light-induced PTT and PDT. (b) Photographs for nude mice bearing HeLa tumors treated with Ru@SWCNTs under 808 nm laser exposure. Reprint from ref. 170 with permission. Copyright 2015, American Chemical Society.

π–π stacking. This as-prepared UCNP-GO/ZnPc theranostic nanoplatform can be used for combinatorial PDT and PTT to inhibit tumor growth.

### Other related nanomaterials

Other nanomaterials, including iron oxide, tungsten oxide nanowires, and copper sulfide NPs, have also been extensively demonstrated to work as effective photosensitive agents in NIR light-controlled therapy.

For example, owing to their robust superparamagnetic property, iron oxide nanostructures are widely used as contrast agents for magnetic resonance imaging (MRI), magnetic bioseparation and magnetic field-guided drug delivery *in vitro* and *in vivo*.[237–239] Recently, Liu and co-workers developed a novel magnetic carrier based on PEGylated iron oxide nanoclusters (IONCs) for delivering PDT reagents to target tumors.[213] In this typical study, one commonly used PS, Ce6, was loaded on the PEG-functionalized IONCs. This IONC-PEG-Ce6 conjugate exhibits significantly accelerated cellular uptake and offers greatly improved photodynamic cancer cell-killing efficiency under NIR light exposure.

Generally, within the entire PDT process, nanostructures are usually carriers for effective delivery of PS molecules into targeted disease areas. One important reason is the hydrophobic property of commonly used PS reagents. Most PS molecules used thus far show low water solubility and poor disease-targeting capability. Conjugation with nanostructures can greatly help to overcome these technical barriers. More importantly, by taking great advantage of other intrinsic properties from the applied nanostructures, such as the super-paramagnetism of iron oxide particles, the upconverting property and high atomic elements in UCNPs, as well as NIR absorbance of carbon-based nanostructures, these PDT nanomaterial complexes also act as integrated platforms to achieve multimodality imaging, such as MRI, biological imaging, CT and photoacoustic imaging[99,161,213,214,219,220,240] for early-stage tumor diagnosis, real-time monitoring of therapy intervention and accomplishment of personalized medicine.

## Conclusion and current challenges

Nanotechnology has been well proved to play an essential role in the light-triggered therapeutic systems. Combining novel nanoscale properties, nanomaterials can provide efficient platforms for integrating diverse functions into a single construct, which indicate that the goal of "one fits all" in cancer treatment may be nearly realized. So far, the use of nanostructures in biomedical applications, especially in cancer diagnosis and therapy, has attracted tremendous interest. In this review, the latest advances in NIR light-controlled therapies based on various NIR-responsive nanomaterials are summarized (see summary of representative examples featured in Table 1). We concentrated primarily on three types of therapeutic strategies: NIR light-mediated drug delivery, NIR light-controlled photothermal therapy and NIR light-based photodynamic therapy.

Among the various modalities for NIR light-controlled therapies, several commonly used nanostructures for such treatments are mainly composed of UCNPs, gold nanomaterials, carbon-based nanomaterials and other related nanostructures. Apart from their attractive biocompatibility as well as good physical and chemical properties, many challenges remain:

(i) NIR light is more biological-friendly not only due to its minimal photodamage to living tissues, but also because it significantly enhanced penetration depth *in vivo*. When used for therapeutic purposes, NIR-light excitations are preferable to irradiation in the UV or visible windows. However, for light-sensitive agents, they usually resort to short-wavelength light with higher energy, especially for the chemical "uncaging" process where bond breaking may occur. For the nanomaterials that can convert NIR light to short-wavelength light (for instance, UCNPs), the quantum yield of the upconversion process is usually low (efficiency <1%). Therefore, development of nanoagents with high photo-converting efficiency is still urgently needed.

(ii) Another key challenge in NIR light-controlled therapy is that most nanomaterials, especially those with inorganic components, are not biodegradable and could potentially be retained inside the body for long periods after treatment. Although numerous *in vitro* and *in vivo* studies have broadly demonstrated that with appropriate surface coatings, there is no noticeable toxicity observed, nanomaterials for biomedical applications are still being cautiously examined to determine long-term safety. In general, thanks to the rapid development of nanotechnologies and tremendous efforts made in this area, final approval for promising theranostic clinical applications based on nanostructures may occur in the near future.

(iii) A variety of modification strategies have been used to improve nanoparticle biocompatibility in living systems. Principal advantages of the nanomaterials discussed in this review, such as gold-based nanomaterials, UCNPs and carbon-related nanostructures, are mostly attributed to their low toxicity, small hydrodynamic size, inert chemical reactivity and multifunctional properties, which have been well recognized as facilitating their unique applications for targeted delivery of PTT, PDT and chemotherapy. Moreover, besides the delivery of anticancer drug molecules, the aforementioned nanomaterials can also be used for the delivery of other therapeutic agents, such as DNA, protein and siRNA. However, like many other inorganic nanomaterials, behaviors of these nanomaterials in biological systems including their probability in causing cytotoxicity, potential immune response, and effective renal clearance still require further investigation.

(iv) The ultimate goal of nanostructure-assisted phototherapies is to maximize therapeutic activity while simultaneously minimizing side effects. In this regard, various approaches for drug delivery, PTT and PDT have already been well established and they have demonstrated great potential in biomedical investigations, especially upon taking advantage of nanostructures. The intrinsic property of nanostructures is always at

**Table 1** Representative examples of nanostructures for NIR light-controlled therapies

| Applications | Type of nanomaterial | | Size | Light wavelength | Toxicity aspect (only nanomaterials) | Ref. |
|---|---|---|---|---|---|---|
| Drug delivery | UCNPs | UCNPs@$SiO_2$ | 50 nm, 35 nm | 980 nm | None | 96, 98 |
| | | UCNPs | 20.1 ± 3.0 nm, 65 nm | 980 nm | None | 97, 99 |
| | | UCNPs@m$SiO_2$ | 75 nm, 80 nm | 980 nm | Cytotoxic for A548 cell line at 64 μg $mL^{-1}$, none | 100, 101 |
| | | UCNPs@Lipo | 18 nm | 980 nm | None | 102 |
| | Gold-based nanostructures | AuNRs@$SiO_2$ | 60 nm, 100 nm (diameters) | 808 nm, 808 nm | None | 28, 111 |
| | | AuNS | 38.5 ± 3.17 nm | 808 nm | None | 114 |
| | | Assembled AuNPs | 5 nm | 980 nm | None | 120 |
| | | AuNCs | 46 nm | 808 nm | None | 122 |
| | | Gold nanostars | 25 nm, 85 nm, 150 nm | 680 nm, 808 nm, 1064 nm | None | 123 |
| | Carbon-based nanomaterials | CNT | 1–2 nm | 808 nm | Minimal cytotoxicity | 137 |
| | | Graphene oxide | <20 nm | 810 nm | None | 139 |
| | Other materials | CuS@m$SiO_2$ | 37 nm | 980 nm | No negative effect on living cells | 140 |
| | | $MoS_2$ | 80 nm | 808 nm | None | 55 |
| Photothermal therapy | UCNPs | UCNPs-CuS | 74.9 nm | 980 nm | No *in vivo* toxicity effect | 152 |
| | | UCNPs-IR825 | 60 nm | 808 nm | None | 40 |
| | Gold-based nanostructures | AuNPs | 26.2 nm | 808 nm | Negligible toxicity | 161 |
| | | AuNPs@SiNWs | 8.69 ± 3.35 nm | 808 nm | To MDA-MB-435 cells | 162 |
| | | AuNRs | 120 nm, 47 nm (diameters) | 800 nm, 810 nm | None, none | 164, 165 |
| | Carbon-based nanomaterials | CNT | 2–5 nm, 10 nm (diameters) | 808 nm, 808 nm | Without toxicity or abnormal behavior for long time | 166, 167 |
| | | Graphene oxide | 10–50 nm | 808 nm | No obvious toxic side effects in 40 days | 171 |
| | Other materials | Black phosphorus | 3 nm | 808 nm | Biodegradable, no *in vivo* toxicity | 174 |
| | | CuS | 11 nm | 808 nm | None | 175 |
| | | Pd nano-sheets | 4.4 nm | 808 nm | No noticeable toxicity in mice *in vivo* | 182 |
| Photodynamic therapy | UCNPs | UCNPs@m$SiO_2$ | 100 nm | 980 nm | None | 215 |
| | | UCNPs | 35 nm, 30 nm | 980 nm, 915 nm | Low toxicity, none | 25, 216 |
| | | Nd-UCNPs | 40 ± 2 nm | 808 nm | None | 229 |
| | Gold-based nanostructures | AuNPs | 5.5 nm | >600 nm | None | 202 |
| | | AuNRs | 37.3 ± 2.4 nm | 915 nm | Without inducing any noticeable side effects *in vivo* | 232 |
| | Carbon-based nanomaterials | CNT | 0.7–1.3 nm (diameters) | 808 nm | No serious toxic effects were observed | 170 |
| | | Graphene oxide | 2–6 nm (diameters) | White light (400–800 nm) | Low cytotoxicity and good biocompatibility | 210 |
| | Other materials | Iron oxide | 100 nm | 704 nm | None | 213 |

the heart of new concepts that meet various therapeutic demands, including drug-loading efficiency, controlled drug release rate, targeting and localized accumulations of therapeutic agents at specific disease areas. Currently, nanostructure-assisted therapies have become the new frontier for medicine and many exciting possibilities have been offered. However, before efficient strategies to tackle demanding technical obstacles emerge, effective therapy based on nanostructures remains an unrealistic niche and there is still a long way to go before FDA recognition to benefit public healthcare systems. In addition, it has been reported that most cancer deaths were caused by the metastatic spread of cancer in which tumour cells escape from the primary tumor and initiate new tumors. Although several works have demonstrated phototheranostic agents for monitoring or treating metastatic sites, many challenges remain and greater effort must be focused on finding suitable NIR phototherapy agents to prevent tumor metastasis. A systematic understanding of relevant oncology pathways is essential to providing important insights in the rational design, new fabrication, and non-invasive evaluation for treatment consequences of nanostructure-based therapeutic platforms *in vitro* and *in vivo*.

Thus far, almost every new element in nanoscale structures has been screened for novel biomedical systems. Optimizing and controlling architectures of the agents are one of the most effective strategies to develop desired therapeutic agents. With the advances in nanostructure chemistry and technology, it is expected that more and more biocompatible nanostructures with well-defined and -controlled functions are likely to become available. Such new members will enrich nanomedicine development and contribute significantly to new generations of therapeutic platforms. While many efforts must be used in the design and synthesis of new nanomaterials, it should be noted that the choice of optimal excitation is also important for NIR light-controlled therapy applications. Beside the first biological NIR window, the second and third biological NIR window have also been studied very recently due to improved tissue penetration and greater spatial resolution,[241–243] which may enhance the new generation of NIR light-responsive phototherapy.

## Acknowledgements

This work was partially supported by start-up grants (SUG), tier 1 (RG 11/13, RG 35/15 and RG 110/16 (S)), Nanyang Technological University, Singapore; the National Natural Science Foundation of China (grants 21405108, 11304214 and 51628201), Jiangsu Provincial Key Laboratory of Radiation Medicine and Protection and the Priority Academic Program Development of Jiangsu Higher Education Institutions (PAPD), China.

## Notes and references

1 H. Koo, M. S. Huh, I. C. Sun, S. H. Yuk, K. Choi, K. Kim and I. C. Kwon, *Acc. Chem. Res.*, 2011, **44**, 1018–1028.
2 J. K. Willmann, N. van Bruggen, L. M. Dinkelborg and S. S. Gambhir, *Nat. Rev. Drug Discovery*, 2008, **7**, 591–607.
3 J. Nicolas, S. Mura, D. Brambilla, N. Mackiewicz and P. Couvreur, *Chem. Soc. Rev.*, 2013, **42**, 1147–1235.
4 C. Li, *Nat. Mater.*, 2014, **13**, 110–115.
5 Y. M. Yang, J. X. Aw, K. Chen, F. Liu, P. Padmanabhan, Y. L. Hou, Z. Cheng and B. G. Xing, *Chem. – Asian J.*, 2011, **6**, 1381–1389.
6 C. L. Zhu, X. Y. Song, W. H. Zhou, H. H. Yang, Y. H. Wen and X. R. Wang, *J. Mater. Chem.*, 2009, **19**, 7765–7770.
7 A. Bansal and Y. Zhang, *Acc. Chem. Res.*, 2014, **47**, 3052–3060.
8 S. Wang, Z. Teng, P. Huang, D. Liu, Y. Liu, Y. Tian, J. Sun, Y. Li, H. Ju, X. Chen and G. Lu, *Small*, 2015, **11**, 1801–1810.
9 Q. Shao and B. Xing, *Chem. Commun.*, 2012, **48**, 1739–1741.
10 V. Biju, *Chem. Soc. Rev.*, 2014, **43**, 744–764.
11 H. Wang, Z. Feng, D. Wu, K. J. Fritzsching, M. Rigney, J. Zhou, Y. Jiang, K. Schmidt-Rohr and B. Xu, *J. Am. Chem. Soc.*, 2016, **138**, 10758–10761.
12 Y. Yang, B. Velmurugan, X. Liu and B. Xing, *Small*, 2013, **9**, 2937–2944.
13 E. S. Shibu, M. Hamada, N. Murase and V. Biju, *J. Photochem. Photobiol., C*, 2013, **15**, 53–72.
14 G. Chen, I. Roy, C. Yang and P. N. Prasad, *Chem. Rev.*, 2016, **116**, 2826–2885.
15 B. Liu, C. Li, Z. Cheng, Z. Hou, S. Huang and J. Lin, *Biomater. Sci.*, 2016, **4**, 890–909.
16 E. Guzman, J. L. Langowski and L. Owen-Schaub, *Apoptosis*, 2003, **8**, 315–325.
17 K. Heil, D. Pearson and T. Carell, *Chem. Soc. Rev.*, 2011, **40**, 4271–4278.
18 J. V. Frangioni, *Curr. Opin. Chem. Biol.*, 2003, **7**, 626–634.
19 H. Kobayashi, M. Ogawa, R. Alford, P. L. Choyke and Y. Urano, *Chem. Rev.*, 2010, **110**, 2620–2640.
20 Y. Yang, J. Mu and B. Xing, *WIREs Nanomed. Nanobiotechnol.*, 2017, **9**, e1408.
21 B. J. Heilman, J. St. John, S. R. J. Oliver and P. K. Mascharak, *J. Am. Chem. Soc.*, 2012, **134**, 11573–11582.
22 J. W. Chung, K. Lee, C. Neikirk, C. M. Nelson and R. D. Priestley, *Small*, 2012, **8**, 1693–1700.
23 Q. Shao and B. Xing, *Chem. Soc. Rev.*, 2010, **39**, 2835–2846.
24 V. Shanmugam, S. Selvakumar and C. S. Yeh, *Chem. Soc. Rev.*, 2014, **43**, 6254–6287.
25 S. Cui, D. Yin, Y. Chen, Y. Di, H. Chen, Y. Ma, S. Achilefu and Y. Gu, *ACS Nano*, 2013, **7**, 676–688.
26 G. Jalani, R. Naccache, D. H. Rosenzweig, L. Haglund, F. Vetrone and M. Cerruti, *J. Am. Chem. Soc.*, 2016, **138**, 1078–1083.
27 M. S. Noh, S. Lee, H. Kang, J. K. Yang, H. Lee, D. Hwang, J. W. Lee, S. Jeong, Y. Jang, B. H. Jun, D. H. Jeong, S. K. Kim, Y. S. Lee and M. H. Cho, *Biomaterials*, 2015, **45**, 81–92.
28 X. J. Yang, X. Liu, Z. Liu, F. Pu, J. S. Ren and X. G. Qu, *Adv. Mater.*, 2012, **24**, 2890–2895.
29 C. Wang, H. Tao, L. Cheng and Z. Liu, *Biomaterials*, 2011, **32**, 6145–6154.

30 G. Yang, R. Lv, F. He, F. Qu, S. Gai, S. Du, Z. Wei and P. Yang, *Nanoscale*, 2015, **7**, 13747–13758.
31 R. Lv, P. Yang, F. He, S. Gai, G. Yang, Y. Dai, Z. Hou and J. Lin, *Biomaterials*, 2015, **63**, 115–127.
32 L. Cheng, C. Wang, L. Feng, K. Yang and Z. Liu, *Chem. Rev.*, 2014, **114**, 10869–10939.
33 S. Shen, S. Wang, R. Zheng, X. Zhu, X. Jiang, D. Fu and W. Yang, *Biomaterials*, 2015, **39**, 67–74.
34 Y. Hu, Y. Yang, H. Wang and H. Du, *ACS Nano*, 2015, **9**, 8744–8754.
35 Y. Min, J. Li, F. Liu, P. Padmanabhan, E. Yeow and B. Xing, *Nanomaterials*, 2014, **4**, 129.
36 S. Mura, J. Nicolas and P. Couvreur, *Nat. Mater.*, 2013, **12**, 991–1003.
37 Y. I. Park, K. T. Lee, Y. D. Suh and T. Hyeon, *Chem. Soc. Rev.*, 2015, **44**, 1302–1317.
38 M.-F. Tsai, S.-H. G. Chang, F.-Y. Cheng, V. Shanmugam, Y.-S. Cheng, C.-H. Su and C.-S. Yeh, *ACS Nano*, 2013, **7**, 5330–5342.
39 N. W. S. Kam, M. O'Connell, J. A. Wisdom and H. Dai, *Proc. Natl. Acad. Sci. U. S. A.*, 2005, **102**, 11600–11605.
40 Q. Chen, C. Wang, L. Cheng, W. He, Z. Cheng and Z. Liu, *Biomaterials*, 2014, **35**, 2915–2923.
41 X. Yang, M. Yang, B. Pang, M. Vara and Y. Xia, *Chem. Rev.*, 2015, **115**, 10410–10488.
42 R. de la Rica, D. Aili and M. M. Stevens, *Adv. Drug Delivery Rev.*, 2012, **64**, 967–978.
43 M. De, P. S. Ghosh and V. M. Rotello, *Adv. Mater.*, 2008, **20**, 4225–4241.
44 D. Peer, J. M. Karp, S. Hong, O. C. FaroKhzad, R. Margalit and R. Langer, *Nat. Nanotechnol.*, 2007, **2**, 751–760.
45 B. Duncan, C. Kim and V. M. Rotello, *J. Controlled Release*, 2010, **148**, 122–127.
46 F. Muharnmad, M. Guo, W. Qi, F. Sun, A. Wang, Y. Guo and G. Zhu, *J. Am. Chem. Soc.*, 2011, **133**, 8778–8781.
47 C. Yaguee, M. Arruebo and J. Santamaria, *Chem. Commun.*, 2010, **46**, 7513–7515.
48 K. Patel, S. Angelos, W. R. Dichtel, A. Coskun, Y.-W. Yang, J. I. Zink and J. F. Stoddart, *J. Am. Chem. Soc.*, 2008, **130**, 2382–2383.
49 C. L. Zhu, C. H. Lu, X. Y. Song, H. H. Yang and X. R. Wang, *J. Am. Chem. Soc.*, 2011, **133**, 1278–1281.
50 J. L. Vivero Escoto, I. I. Slowing, C. W. Wu and V. S. Y. Lin, *J. Am. Chem. Soc.*, 2009, **131**, 3462–3463.
51 Z. Cheng, A. Al Zaki, J. Z. Hui, V. R. Muzykantov and A. Tsourkas, *Science*, 2012, **338**, 903–910.
52 S. Mura and P. Couvreur, *Adv. Drug Delivery Rev.*, 2012, **64**, 1394–1416.
53 T. L. Doane and C. Burda, *Chem. Soc. Rev.*, 2012, **41**, 2885–2911.
54 Y. Yang, F. Liu, X. Liu and B. Xing, *Nanoscale*, 2013, **5**, 231–238.
55 W. Yin, L. Yan, J. Yu, G. Tian, L. Zhou, X. Zheng, X. Zhang, Y. Yong, J. Li, Z. Gu and Y. Zhao, *ACS Nano*, 2014, **8**, 6922–6933.
56 J. L. Vivero Escoto, R. C. Huxford Phillips and W. B. Lin, *Chem. Soc. Rev.*, 2012, **41**, 2673–2685.
57 G. Liu and C.-M. Dong, *Biomacromolecules*, 2012, **13**, 1573–1583.
58 S. Kumar, J.-F. Allard, D. Morris, Y. L. Dory, M. Lepage and Y. Zhao, *J. Mater. Chem.*, 2012, **22**, 7252–7257.
59 J. Jiang, X. Tong and Y. Zhao, *J. Am. Chem. Soc.*, 2005, **127**, 8290–8291.
60 Q. Jin, F. Mitschang and S. Agarwal, *Biomacromolecules*, 2011, **12**, 3684–3691.
61 S. Karthik, N. Puvvada, B. N. P. Kumar, S. Rajput, A. Pathak, M. Mandal and N. D. P. Singh, *ACS Appl. Mater. Interfaces*, 2013, **5**, 5232–5238.
62 G. M. Dubowchik, R. A. Firestone, L. Padilla, D. Willner, S. J. Hofstead, K. Mosure, J. O. Knipe, S. J. Lasch and P. A. Trail, *Bioconjugate Chem.*, 2002, **13**, 855–869.
63 F. Auzel, *Chem. Rev.*, 2004, **104**, 139–174.
64 F. Wang, D. Banerjee, Y. Liu, X. Chen and X. Liu, *Analyst*, 2010, **135**, 1839–1854.
65 D. Yang, P. a. Ma, Z. Hou, Z. Cheng, C. Li and J. Lin, *Chem. Soc. Rev.*, 2015, **44**, 1416–1448.
66 J. Zhou, Q. Liu, W. Feng, Y. Sun and F. Li, *Chem. Rev.*, 2015, **115**, 395–465.
67 F. Wang, Y. Han, C. S. Lim, Y. Lu, J. Wang, J. Xu, H. Chen, C. Zhang, M. Hong and X. Liu, *Nature*, 2010, **463**, 1061–1065.
68 F. Wang and X. Liu, *Chem. Soc. Rev.*, 2009, **38**, 976–989.
69 M.-F. Joubert, *Opt. Mater.*, 1999, **11**, 181–203.
70 X. Li, F. Zhang and D. Zhao, *Chem. Soc. Rev.*, 2015, **44**, 1346–1378.
71 X. Liu, R. Deng, Y. Zhang, Y. Wang, H. Chang, L. Huang and X. Liu, *Chem. Soc. Rev.*, 2015, **44**, 1479–1508.
72 H. Dong, L.-D. Sun and C.-H. Yan, *Chem. Soc. Rev.*, 2015, **44**, 1608–1634.
73 D. K. Chatterjee, A. J. Rufaihah and Y. Zhang, *Biomaterials*, 2008, **29**, 937–943.
74 R. Abdul Jalil and Y. Zhang, *Biomaterials*, 2008, **29**, 4122–4128.
75 L.-L. Li, R. Zhang, L. Yin, K. Zheng, W. Qin, P. R. Selvin and Y. Lu, *Angew. Chem.*, 2012, **124**, 6225–6229.
76 F. Liu, Q. Zhao, H. You and Z. Wang, *Nanoscale*, 2013, **5**, 1047–1053.
77 S. H. C. Askes, N. L. Mora, R. Harkes, R. I. Koning, B. Koster, T. Schmidt, A. Kros and S. Bonnet, *Chem. Commun.*, 2015, **51**, 9137–9140.
78 R. Wang and F. Zhang, *J. Mater. Chem. B*, 2014, **2**, 2422–2443.
79 F. C. J. M. van Veggel, C. Dong, N. J. J. Johnson and J. Pichaandi, *Nanoscale*, 2012, **4**, 7309–7321.
80 N. M. Idris, Z. Li, L. Ye, E. K. W. Sim, R. Mahendran, P. C.-L. Ho and Y. Zhang, *Biomaterials*, 2009, **30**, 5104–5113.
81 L.-Q. Xiong, Z.-G. Chen, M.-X. Yu, F.-Y. Li, C. Liu and C.-H. Huang, *Biomaterials*, 2009, **30**, 5592–5600.
82 L. Cheng, K. Yang, M. Shao, S.-T. Lee and Z. Liu, *J. Phys. Chem. C*, 2011, **115**, 2686–2692.

 

83 J. Zhou, Z. Liu and F. Li, *Chem. Soc. Rev.*, 2012, **41**, 1323–1349.
84 S.-H. Tang, J. Wang, C.-X. Yang, L.-X. Dong, D. Kong and X.-P. Yan, *Nanoscale*, 2014, **6**, 8037–8044.
85 L. Zhou, B. He, J. Huang, Z. Cheng, X. Xu and C. Wei, *ACS Appl. Mater. Interfaces*, 2014, **6**, 7719–7727.
86 U. Rocha, C. Jacinto da Silva, W. Ferreira Silva, I. Guedes, A. Benayas, L. Martínez Maestro, M. Acosta Elias, E. Bovero, F. C. J. M. van Veggel, J. A. García Solé and D. Jaque, *ACS Nano*, 2013, **7**, 1188–1199.
87 Y. Zhang, F. Zheng, T. Yang, W. Zhou, Y. Liu, N. Man, L. Zhang, N. Jin, Q. Dou, Y. Zhang, Z. Li and L.-P. Wen, *Nat. Mater.*, 2012, **11**, 817–826.
88 R. Deng, X. Xie, M. Vendrell, Y.-T. Chang and X. Liu, *J. Am. Chem. Soc.*, 2011, **133**, 20168–20171.
89 Y. Wang, P. Shen, C. Li, Y. Wang and Z. Liu, *Anal. Chem.*, 2012, **84**, 1466–1473.
90 Y. Wang, Z. Wu and Z. Liu, *Anal. Chem.*, 2013, **85**, 258–264.
91 J. G. Jesu Raj, M. Quintanilla, K. A. Mahmoud, A. Ng, F. Vetrone and M. Zourob, *ACS Appl. Mater. Interfaces*, 2015, **7**, 18257–18265.
92 M. Kumar and P. Zhang, *Langmuir*, 2009, **25**, 6024–6027.
93 Y. Liu, T. Kobayashi, M. Iizuka, T. Tanaka, I. Sotokawa, A. Shimoyama, Y. Murayama, E. Otsuji, S.-i. Ogura and H. Yuasa, *Bioorg. Med. Chem.*, 2013, **21**, 2832–2842.
94 H. Liu, Y. Fu, Y. Li, Z. Ren, X. Li, G. Han and C. Mao, *Langmuir*, 2016, **32**, 9083–9090.
95 G. Chen, H. Qiu, P. N. Prasad and X. Chen, *Chem. Rev.*, 2014, **114**, 5161–5214.
96 Y. M. Yang, Q. Shao, R. R. Deng, C. Wang, X. Teng, K. Cheng, Z. Cheng, L. Huang, Z. Liu, X. G. Liu and B. G. Xing, *Angew. Chem., Int. Ed.*, 2012, **51**, 3125–3129.
97 L. L. Fedoryshin, A. J. Tavares, E. Petryayeva, S. Doughan and U. J. Krull, *ACS Appl. Mater. Interfaces*, 2014, **6**, 13600–13606.
98 Y. Min, J. Li, F. Liu, E. K. L. Yeow and B. Xing, *Angew. Chem., Int. Ed.*, 2014, **53**, 1012–1016.
99 Y. Dai, H. Xiao, J. Liu, Q. Yuan, P. a. Ma, D. Yang, C. Li, Z. Cheng, Z. Hou, P. Yang and J. Lin, *J. Am. Chem. Soc.*, 2013, **135**, 18920–18929.
100 H. Wang, R.-l. Han, L.-m. Yang, J.-h. Shi, Z.-j. Liu, Y. Hu, Y. Wang, S.-j. Liu and Y. Gan, *ACS Appl. Mater. Interfaces*, 2016, **8**, 4416–4423.
101 M. K. G. Jayakumar, N. M. Idris and Y. Zhang, *Proc. Natl. Acad. Sci. U. S. A.*, 2012, **109**, 8483–8488.
102 C. Yao, P. Wang, X. Li, X. Hu, J. Hou, L. Wang and F. Zhang, *Adv. Mater.*, 2016, **28**, 9341–9348.
103 W. I. Choi, J. Y. Kim, C. Kang, C. C. Byeon, Y. H. Kim and G. Tae, *ACS Nano*, 2011, **5**, 1995–2003.
104 W. Lu, M. P. Melancon, C. Xiong, Q. Huang, A. Elliott, S. Song, R. Zhang, L. G. Flores, J. G. Gelovani, L. V. Wang, G. Ku, R. J. Stafford and C. Li, *Cancer Res.*, 2011, **71**, 6116–6121.
105 J. Chen, C. Glaus, R. Laforest, Q. Zhang, M. Yang, M. Gidding, M. J. Welch and Y. Xia, *Small*, 2010, **6**, 811–817.
106 S.-W. Lv, Y. Liu, M. Xie, J. Wang, X.-W. Yan, Z. Li, W.-G. Dong and W.-H. Huang, *ACS Nano*, 2016, **10**, 6201–6210.
107 J. Qiu and W. D. Wei, *J. Phys. Chem. C*, 2014, **118**, 20735–20749.
108 H. Kim, K. Chung, S. Lee, D. H. Kim and H. Lee, *WIREs Nanomed. Nanobiotechnol.*, 2016, **8**, 23–45.
109 A. Barhoumi, R. Huschka, R. Bardhan, M. W. Knight and N. J. Halas, *Chem. Phys. Lett.*, 2009, **482**, 171–179.
110 Y. T. Chang, P. Y. Liao, H. S. Sheu, Y. J. Tseng, F. Y. Cheng and C. S. Yeh, *Adv. Mater.*, 2012, **24**, 3309–3314.
111 Z. Zhang, J. Wang, X. Nie, T. Wen, Y. Ji, X. Wu, Y. Zhao and C. Chen, *J. Am. Chem. Soc.*, 2014, **136**, 7317–7326.
112 R. Huschka, A. Barhoumi, Q. Liu, J. A. Roth, L. Ji and N. J. Halas, *ACS Nano*, 2012, **6**, 7681–7691.
113 E. H. Jeong, J. H. Ryu, H. Jeong, B. Jang, H. Y. Lee, S. Hong, H. Lee and H. Lee, *Chem. Commun.*, 2014, **50**, 13388–13390.
114 J. You, G. Zhang and C. Li, *ACS Nano*, 2010, **4**, 1033–1041.
115 X. Liu, H. Huang, Q. Jin and J. Ji, *Langmuir*, 2011, **27**, 5242–5251.
116 J. H. Heo, K.-I. Kim, H. H. Cho, J. W. Lee, B. S. Lee, S. Yoon, K. J. Park, S. Lee, J. Kim, D. Whang and J. H. Lee, *Langmuir*, 2015, **31**, 13773–13782.
117 J. Nam, N. Won, H. Jin, H. Chung and S. Kim, *J. Am. Chem. Soc.*, 2009, **131**, 13639–13645.
118 H. Li, X. Liu, N. Huang, K. Ren, Q. Jin and J. Ji, *ACS Appl. Mater. Interfaces*, 2014, **6**, 18930–18937.
119 Y. Xia, X. Wu, J. Zhao, J. Zhao, Z. Li, W. Ren, Y. Tian, A. Li, Z. Shen and A. Wu, *Nanoscale*, 2016, **8**, 18682–18692.
120 N. Niu, F. He, P. a. Ma, S. Gai, G. Yang, F. Qu, Y. Wang, J. Xu and P. Yang, *ACS Appl. Mater. Interfaces*, 2014, **6**, 3250–3262.
121 M. S. Yavuz, Y. Cheng, J. Chen, C. M. Cobley, Q. Zhang, M. Rycenga, J. Xie, C. Kim, K. H. Song, A. G. Schwartz, L. V. Wang and Y. Xia, *Nat. Mater.*, 2009, **8**, 935–939.
122 T. Sun, Y. Wang, Y. Wang, J. Xu, X. Zhao, S. Vangveravong, R. H. Mach and Y. Xia, *Adv. Healthcare Mater.*, 2014, **3**, 1283–1291.
123 A. Espinosa, A. K. A. Silva, A. Sánchez-Iglesias, M. Grzelczak, C. Péchoux, K. Desboeufs, L. M. Liz-Marzán and C. Wilhelm, *Adv. Healthcare Mater.*, 2016, **5**, 1040–1048.
124 G. Hong, S. Diao, A. L. Antaris and H. Dai, *Chem. Rev.*, 2015, **115**, 10816–10906.
125 K. Shi, Z. Liu, Y.-Y. Wei, W. Wang, X.-J. Ju, R. Xie and L.-Y. Chu, *ACS Appl. Mater. Interfaces*, 2015, **7**, 27289–27298.
126 B. S. Wong, S. L. Yoong, A. Jagusiak, T. Panczyk, H. K. Ho, W. H. Ang and G. Pastorin, *Adv. Drug Delivery Rev.*, 2013, **65**, 1964–2015.
127 Q. He, D. O. Kiesewetter, Y. Qu, X. Fu, J. Fan, P. Huang, Y. Liu, G. Zhu, Y. Liu, Z. Qian and X. Chen, *Adv. Mater.*, 2015, **27**, 6741–6746.
128 S. H. Kim, J. E. Lee, S. M. Sharker, J. H. Jeong, I. In and S. Y. Park, *Biomacromolecules*, 2015, **16**, 3519–3529.

129 Y. Hashida, H. Tanaka, S. Zhou, S. Kawakami, F. Yamashita, T. Murakami, T. Umeyama, H. Imahori and M. Hashida, *J. Controlled Release*, 2014, **173**, 59–66.
130 Z. Cheng, R. Chai, P. Ma, Y. Dai, X. Kang, H. Lian, Z. Hou, C. Li and J. Lin, *Langmuir*, 2013, **29**, 9573–9580.
131 J. Fan, N. He, Q. He, Y. Liu, Y. Ma, X. Fu, Y. Liu, P. Huang and X. Chen, *Nanoscale*, 2015, **7**, 20055–20062.
132 F. F. N. Luís, J. K. John, D. V. R. Brent, R. Rajagopal, E. R. Daniel and G. H. Roger, *Nanotechnology*, 2013, **24**, 375104.
133 T. Igarashi, H. Kawai, K. Yanagi, N. T. Cuong, S. Okada and T. Pichler, *Phys. Rev. Lett.*, 2015, **114**, 176807.
134 G. V. Hartland, *Chem. Rev.*, 2011, **111**, 3858–3887.
135 J. T. Robinson, G. Hong, Y. Liang, B. Zhang, O. K. Yaghi and H. Dai, *J. Am. Chem. Soc.*, 2012, **134**, 10664–10669.
136 C. Liang, S. Diao, C. Wang, H. Gong, T. Liu, G. Hong, X. Shi, H. Dai and Z. Liu, *Adv. Mater.*, 2014, **26**, 5646–5652.
137 Y. Qin, J. Chen, Y. Bi, X. Xu, H. Zhou, J. Gao, Y. Hu, Y. Zhao and Z. Chai, *Acta Biomater.*, 2015, **17**, 201–209.
138 W. Zhang, Z. Guo, D. Huang, Z. Liu, X. Guo and H. Zhong, *Biomaterials*, 2011, **32**, 8555–8561.
139 P. Matteini, F. Tatini, L. Cavigli, S. Ottaviano, G. Ghini and R. Pini, *Nanoscale*, 2014, **6**, 7947–7953.
140 X. Liu, Q. Ren, F. Fu, R. Zou, Q. Wang, G. Xin, Z. Xiao, X. Huang, Q. Liu and J. Hu, *Dalton Trans.*, 2015, **44**, 10343–10351.
141 J. Lee, J. Kim and W. J. Kim, *Chem. Mater.*, 2016, **28**, 6417–6424.
142 J. N. Coleman, M. Lotya, A. O'Neill, S. D. Bergin, P. J. King, U. Khan, K. Young, A. Gaucher, S. De and R. J. Smith, *Science*, 2011, **331**, 568–571.
143 X. Huang, P. K. Jain, I. H. El-Sayed and M. A. El-Sayed, *Nanomedicine*, 2007, **2**, 681–693.
144 S. Sortino, *J. Mater. Chem.*, 2012, **22**, 301–318.
145 Z. Zhang, J. Wang and C. Chen, *Adv. Mater.*, 2013, **25**, 3869–3880.
146 W. Yang, W. Guo, W. Le, G. Lv, F. Zhang, L. Shi, X. Wang, J. Wang, S. Wang, J. Chang and B. Zhang, *ACS Nano*, 2016, **10**, 10245–10257.
147 J. Han, H. Xia, Y. Wu, S. N. Kong, A. Deivasigamani, R. Xu, K. M. Hui and Y. Kang, *Nanoscale*, 2016, **8**, 7861–7865.
148 R. Vankayala, C.-C. Lin, P. Kalluru, C.-S. Chiang and K. C. Hwang, *Biomaterials*, 2014, **35**, 5527–5538.
149 M. Lin, Y. Gao, F. Hornicek, F. Xu, T. J. Lu, M. Amiji and Z. Duan, *Adv. Colloid Interface Sci.*, 2015, **226**(part B), 123–137.
150 B. Dong, S. Xu, J. Sun, S. Bi, D. Li, X. Bai, Y. Wang, L. Wang and H. Song, *J. Mater. Chem.*, 2011, **21**, 6193–6200.
151 M. Challenor, P. Gong, D. Lorenser, M. Fitzgerald, S. Dunlop, D. D. Sampson and K. Swaminathan Iyer, *ACS Appl. Mater. Interfaces*, 2013, **5**, 7875–7880.
152 Q. Xiao, X. Zheng, W. Bu, W. Ge, S. Zhang, F. Chen, H. Xing, Q. Ren, W. Fan, K. Zhao, Y. Hua and J. Shi, *J. Am. Chem. Soc.*, 2013, **135**, 13041–13048.
153 M. Mitsunaga, M. Ogawa, N. Kosaka, L. T. Rosenblum, P. L. Choyke and H. Kobayashi, *Nat. Med.*, 2011, **17**, 1685–1691.
154 W. Zou, C. Visser, J. A. Maduro, M. S. Pshenichnikov and J. C. Hummelen, *Nat. Photonics*, 2012, **6**, 560–564.
155 F. Ai, Q. Ju, X. Zhang, X. Chen, F. Wang and G. Zhu, *Sci. Rep.*, 2015, **5**, 10785.
156 B. Liu, C. Li, B. Xing, P. Yang and J. Lin, *J. Mater. Chem. B*, 2016, **4**, 4884–4894.
157 C. M. Pitsillides, E. K. Joe, X. B. Wei, R. R. Anderson and C. P. Lin, *Biophys. J.*, 2003, **84**, 4023–4032.
158 A. M. Gobin, E. M. Watkins, E. Quevedo, V. L. Colvin and J. L. West, *Small*, 2010, **6**, 745–752.
159 Z. Wu, X. Lin, Y. Wu, T. Si, J. Sun and Q. He, *ACS Nano*, 2014, **8**, 6097–6105.
160 A. Hatef and M. Meunier, *Opt. Express*, 2015, **23**, 1967–1980.
161 P. Huang, J. Lin, W. Li, P. Rong, Z. Wang, S. Wang, X. Wang, X. Sun, M. Aronova, G. Niu, R. D. Leapman, Z. Nie and X. Chen, *Angew. Chem., Int. Ed.*, 2013, **52**, 13958–13964.
162 Y. Su, X. Wei, F. Peng, Y. Zhong, Y. Lu, S. Su, T. Xu, S.-T. Lee and Y. He, *Nano Lett.*, 2012, **12**, 1845–1850.
163 N. R. Jana, L. Gearheart and C. J. Murphy, *J. Phys. Chem. B*, 2001, **105**, 4065–4067.
164 X. Huang, I. H. El-Sayed, W. Qian and M. A. El-Sayed, *J. Am. Chem. Soc.*, 2006, **128**, 2115–2120.
165 G. von Maltzahn, J.-H. Park, A. Agrawal, N. K. Bandaru, S. K. Das, M. J. Sailor and S. N. Bhatia, *Cancer Res.*, 2009, **69**, 3892–3900.
166 H. K. Moon, S. H. Lee and H. C. Choi, *ACS Nano*, 2009, **3**, 3707–3713.
167 B. Zhang, H. Wang, S. Shen, X. She, W. Shi, J. Chen, Q. Zhang, Y. Hu, Z. Pang and X. Jiang, *Biomaterials*, 2016, **79**, 46–55.
168 Z. Lin, Y. Liu, X. Ma, S. Hu, J. Zhang, Q. Wu, W. Ye, S. Zhu, D. Yang and D. Qu, *Sci. Rep.*, 2015, **5**, 11709.
169 T. Murakami, H. Nakatsuji, M. Inada, Y. Matoba, T. Umeyama, M. Tsujimoto, S. Isoda, M. Hashida and H. Imahori, *J. Am. Chem. Soc.*, 2012, **134**, 17862–17865.
170 P. Zhang, H. Huang, J. Huang, H. Chen, J. Wang, K. Qiu, D. Zhao, L. Ji and H. Chao, *ACS Appl. Mater. Interfaces*, 2015, **7**, 23278–23290.
171 K. Yang, S. Zhang, G. Zhang, X. Sun, S.-T. Lee and Z. Liu, *Nano Lett.*, 2010, **10**, 3318–3323.
172 O. I. Joshua, A. S. Gary, S. J. v. d. Z. Herre and C.-G. Andres, *2D Mater.*, 2015, **2**, 011002.
173 X. Ling, H. Wang, S. Huang, F. Xia and M. S. Dresselhaus, *Proc. Natl. Acad. Sci. U. S. A.*, 2015, **112**, 4523–4530.
174 J. Shao, H. Xie, H. Huang, Z. Li, Z. Sun, Y. Xu, Q. Xiao, X.-F. Yu, Y. Zhao, H. Zhang, H. Wang and P. K. Chu, *Nat. Commun.*, 2016, **7**, 12967.
175 M. Zhou, R. Zhang, M. Huang, W. Lu, S. Song, M. P. Melancon, M. Tian, D. Liang and C. Li, *J. Am. Chem. Soc.*, 2010, **132**, 15351–15358.

 

176 Y. Zhang, Z. Hou, Y. Ge, K. Deng, B. Liu, X. Li, Q. Li, Z. Cheng, P. a. Ma, C. Li and J. Lin, *ACS Appl. Mater. Interfaces*, 2015, **7**, 20696–20706.
177 Q. Tian, M. Tang, Y. Sun, R. Zou, Z. Chen, M. Zhu, S. Yang, J. Wang, J. Wang and J. Hu, *Adv. Mater.*, 2011, **23**, 3542–3547.
178 C. M. Hessel, V. P. Pattani, M. Rasch, M. G. Panthani, B. Koo, J. W. Tunnell and B. A. Korgel, *Nano Lett.*, 2011, **11**, 2560–2566.
179 W. Li, R. Zamani, P. Rivera Gil, B. Pelaz, M. Ibáñez, D. Cadavid, A. Shavel, R. A. Alvarez-Puebla, W. J. Parak, J. Arbiol and A. Cabot, *J. Am. Chem. Soc.*, 2013, **135**, 7098–7101.
180 Q. Tian, J. Hu, Y. Zhu, R. Zou, Z. Chen, S. Yang, R. Li, Q. Su, Y. Han and X. Liu, *J. Am. Chem. Soc.*, 2013, **135**, 8571–8577.
181 X. Huang, S. Tang, X. Mu, Y. Dai, G. Chen, Z. Zhou, F. Ruan, Z. Yang and N. Zheng, *Nat. Nanotechnol.*, 2011, **6**, 28–32.
182 S. Shi, Y. Huang, X. Chen, J. Weng and N. Zheng, *ACS Appl. Mater. Interfaces*, 2015, **7**, 14369–14375.
183 W. Fang, S. Tang, P. Liu, X. Fang, J. Gong and N. Zheng, *Small*, 2012, **8**, 3816–3822.
184 W. Fang, J. Yang, J. Gong and N. Zheng, *Adv. Funct. Mater.*, 2012, **22**, 842–848.
185 S. Tang, X. Huang and N. Zheng, *Chem. Commun.*, 2011, **47**, 3948–3950.
186 L. Tong, C.-C. Chuang, S. Wu and L. Zuo, *Cancer Lett.*, 2015, **367**, 18–25.
187 A. Weidinger and A. Kozlov, *Biomolecules*, 2015, **5**, 472.
188 X. Wei, W. Wang and K. Chen, *J. Phys. Chem. C*, 2013, **117**, 23716–23729.
189 Y. Shen, A. J. Shuhendler, D. Ye, J.-J. Xu and H.-Y. Chen, *Chem. Soc. Rev.*, 2016, **45**, 6725–6741.
190 S. Tachikawa, S. Sato, H. Hazama, Y. Kaneda, K. Awazu and H. Nakamura, *Bioorg. Med. Chem.*, 2015, **23**, 7578–7584.
191 A. Yuan, X. Tang, X. Qiu, K. Jiang, J. Wu and Y. Hu, *Chem. Commun.*, 2015, **51**, 3340–3342.
192 G. Saravanakumar, J. Lee, J. Kim and W. J. Kim, *Chem. Commun.*, 2015, **51**, 9995–9998.
193 J. Tian, L. Ding, H. Ju, Y. Yang, X. Li, Z. Shen, Z. Zhu, J.-S. Yu and C. J. Yang, *Angew. Chem., Int. Ed.*, 2014, **53**, 9544–9549.
194 S. Wang, F. Yuan, K. Chen, G. Chen, K. Tu, H. Wang and L.-Q. Wang, *Biomacromolecules*, 2015, **16**, 2693–2700.
195 S. Li, K. Chang, K. Sun, Y. Tang, N. Cui, Y. Wang, W. Qin, H. Xu and C. Wu, *ACS Appl. Mater. Interfaces*, 2016, **8**, 3624–3634.
196 X. Song, C. Liang, H. Gong, Q. Chen, C. Wang and Z. Liu, *Small*, 2015, **11**, 3932–3941.
197 X. Ding and B.-H. Han, *Angew. Chem., Int. Ed.*, 2015, **54**, 6536–6539.
198 P. Zhang, W. Steelant, M. Kumar and M. Scholfield, *J. Am. Chem. Soc.*, 2007, **129**, 4526–4527.
199 M. Wang, Z. Chen, W. Zheng, H. Zhu, S. Lu, E. Ma, D. Tu, S. Zhou, M. Huang and X. Chen, *Nanoscale*, 2014, **6**, 8274–8282.
200 M. K. Gnanasammandhan, N. M. Idris, A. Bansal, K. Huang and Y. Zhang, *Nat. Protocols*, 2016, **11**, 688–713.
201 Z. Hou, K. Deng, C. Li, X. Deng, H. Lian, Z. Cheng, D. Jin and J. Lin, *Biomaterials*, 2016, **101**, 32–46.
202 Y. Cheng, T. L. Doane, C.-H. Chuang, A. Ziady and C. Burda, *Small*, 2014, **10**, 1799–1804.
203 Y. Yang, Y. Hu, H. Du and H. Wang, *Chem. Commun.*, 2014, **50**, 7287–7290.
204 L. Gao, R. Liu, F. Gao, Y. Wang, X. Jiang and X. Gao, *ACS Nano*, 2014, **8**, 7260–7271.
205 M. Zhang, T. Murakami, K. Ajima, K. Tsuchida, A. S. D. Sandanayaka, O. Ito, S. Iijima and M. Yudasaka, *Proc. Natl. Acad. Sci. U. S. A.*, 2008, **105**, 14773–14778.
206 S. Erbas, A. Gorgulu, M. Kocakusakogullari and E. U. Akkaya, *Chem. Commun.*, 2009, 4956–4958.
207 L. Wang, J. Shi, R. Liu, Y. Liu, J. Zhang, X. Yu, J. Gao, C. Zhang and Z. Zhang, *Nanoscale*, 2014, **6**, 4642–4651.
208 Z. Zhu, Z. Tang, J. A. Phillips, R. Yang, H. Wang and W. Tan, *J. Am. Chem. Soc.*, 2008, **130**, 10856–10857.
209 S. P. Jovanović, Z. Syrgiannis, Z. M. Marković, A. Bonasera, D. P. Kepić, M. D. Budimir, D. D. Milivojević, V. D. Spasojević, M. D. Dramićanin, V. B. Pavlović and B. M. Todorović Marković, *ACS Appl. Mater. Interfaces*, 2015, **7**, 25865–25874.
210 J. Ge, M. Lan, B. Zhou, W. Liu, L. Guo, H. Wang, Q. Jia, G. Niu, X. Huang, H. Zhou, X. Meng, P. Wang, C.-S. Lee, W. Zhang and X. Han, *Nat. Commun.*, 2014, **5**, 4596.
211 J. Qian, D. Wang, F. Cai, Q. Zhan, Y. Wang and S. He, *Biomaterials*, 2012, **33**, 4851–4860.
212 Z. X. Zhao, Y. Z. Huang, S. G. Shi, S. H. Tang, D. H. Li and X. L. Chen, *Nanotechnology*, 2014, **25**, 285701.
213 Z. Li, C. Wang, L. Cheng, H. Gong, S. Yin, Q. Gong, Y. Li and Z. Liu, *Biomaterials*, 2013, **34**, 9160–9170.
214 X. Zhao, Z. Chen, H. Zhao, D. Zhang, L. Tao and M. Lan, *RSC Adv.*, 2014, **4**, 62153–62159.
215 N. M. Idris, M. K. Gnanasammandhan, J. Zhang, P. C. Ho, R. Mahendran and Y. Zhang, *Nat. Med.*, 2012, **18**, 1580–1585.
216 Y. Huang, Q. Xiao, H. Hu, K. Zhang, Y. Feng, F. Li, J. Wang, X. Ding, J. Jiang, Y. Li, L. Shi and H. Lin, *Small*, 2016, **12**, 4200–4210.
217 V. H. Fingar, T. J. Wieman, S. A. Wiehle and P. B. Cerrito, *Cancer Res.*, 1992, **52**, 4914–4921.
218 M. I. Koukourakis, A. Giatromanolaki, J. Skarlatos, L. Corti, S. Blandamura, M. Piazza, K. C. Gatter and A. L. Harris, *Cancer Res.*, 2001, **61**, 1830–1832.
219 Y. Liu, Y. Liu, W. Bu, C. Cheng, C. Zuo, Q. Xiao, Y. Sun, D. Ni, C. Zhang, J. Liu and J. Shi, *Angew. Chem., Int. Ed.*, 2015, **54**, 8105–8109.
220 S. Lu, D. Tu, P. Hu, J. Xu, R. Li, M. Wang, Z. Chen, M. Huang and X. Chen, *Angew. Chem., Int. Ed.*, 2015, **54**, 7915–7919.
221 W. Fan, W. Bu and J. Shi, *Adv. Mater.*, 2016, **28**, 3987–4011.

222 Q. Zhan, J. Qian, H. Liang, G. Somesfalean, D. Wang, S. He, Z. Zhang and S. Andersson-Engels, *ACS Nano*, 2011, **5**, 3744–3757.
223 Y. F. Wang, G. Y. Liu, L. D. Sun, J. W. Xiao, J. C. Zhou and C. H. Yan, *ACS Nano*, 2013, **7**, 7200–7206.
224 Y. Li, J. Tang, D.-X. Pan, L.-D. Sun, C. Chen, Y. Liu, Y.-F. Wang, S. Shi and C.-H. Yan, *ACS Nano*, 2016, **10**, 2766–2773.
225 B. Xu, X. Zhang, W. Huang, Y. Yang, Y. Ma, Z. Gu, T. Zhai and Y. Zhao, *J. Mater. Chem. B*, 2016, **4**, 2776–2784.
226 J. Shen, G. Chen, A. M. Vu, W. Fan, O. S. Bilsel, C. C. Chang and G. Han, *Adv. Opt. Mater.*, 2013, **1**, 644–650.
227 X. Xie, N. Gao, R. Deng, Q. Sun, Q.-H. Xu and X. Liu, *J. Am. Chem. Soc.*, 2013, **135**, 12608–12611.
228 G. Chen, H. Agren, T. Y. Ohulchanskyy and P. N. Prasad, *Chem. Soc. Rev.*, 2015, **44**, 1680–1713.
229 X. Ai, C. J. H. Ho, J. Aw, A. B. E. Attia, J. Mu, Y. Wang, X. Wang, Y. Wang, X. Liu, H. Chen, M. Gao, X. Chen, E. K. L. Yeow, G. Liu, M. Olivo and B. Xing, *Nat. Commun.*, 2016, **7**, 10432.
230 W.-S. Kuo, C.-N. Chang, Y.-T. Chang, M.-H. Yang, Y.-H. Chien, S.-J. Chen and C.-S. Yeh, *Angew. Chem., Int. Ed.*, 2010, **49**, 2711–2715.
231 Y. Xu, R. He, D. Lin, M. Ji and J. Chen, *Nanoscale*, 2015, **7**, 2433–2441.
232 R. Vankayala, Y.-K. Huang, P. Kalluru, C.-S. Chiang and K. C. Hwang, *Small*, 2014, **10**, 1612–1622.
233 V. Pierroz, T. Joshi, A. Leonidova, C. Mari, J. Schur, I. Ott, L. Spiccia, S. Ferrari and G. Gasser, *J. Am. Chem. Soc.*, 2012, **134**, 20376–20387.
234 L. Zhou, W. Wang, J. Tang, J.-H. Zhou, H.-J. Jiang and J. Shen, *Chem. – Eur. J.*, 2011, **17**, 12084–12091.
235 A. Sahu, W. I. Choi, J. H. Lee and G. Tae, *Biomaterials*, 2013, **34**, 6239–6248.
236 Y. Wang, H. Wang, D. Liu, S. Song, X. Wang and H. Zhang, *Biomaterials*, 2013, **34**, 7715–7724.
237 H. W. Gu, P. L. Ho, K. W. T. Tsang, L. Wang and B. Xu, *J. Am. Chem. Soc.*, 2003, **125**, 15702–15703.
238 J. Xie, J. Huang, X. Li, S. Sun and X. Chen, *Curr. Med. Chem.*, 2009, **16**, 1278–1294.
239 Y. Pan, M. J. C. Long, H.-C. Lin, L. Hedstrom and B. Xu, *Chem. Sci.*, 2012, **3**, 3495–3499.
240 J. Bartelmess, S. J. Quinn and S. Giordani, *Chem. Soc. Rev.*, 2015, **44**, 4672–4698.
241 H. Gong, R. Peng and Z. Liu, *Adv. Drug Delivery Rev.*, 2013, **65**, 1951–1963.
242 S. Xu, J. Cui and L. Wang, *TrAC, Trends Anal. Chem.*, 2016, **80**, 149–155.
243 G. Hong, J. C. Lee, J. T. Robinson, U. Raaz, L. Xie, N. F. Huang, J. P. Cooke and H. Dai, *Nat. Med.*, 2012, **18**, 1841–1846.

 